HOW WELL DO ERA-INTERIM AND MERRA-2 CAPTURE ITCZ CHARACTERISTICS AND PRECIPITATION?

A Thesis

by

COREY STORM HOWARD

Submitted to the Office of Graduate and Professional Studies of
Texas A&M University
in partial fulfillment of the requirements for the degree of

MASTER OF SCIENCE

Chair of Committee,	Anita D. Rapp
Committee Members,	Christopher Nowotarski
	Andrew Klein
Head of Department,	Ping Yang

August 2018

Major Subject: Atmospheric Science

ABSTRACT

The Intertropical Convergence Zone (ITCZ) is one of the most important features of the tropical atmosphere. Recent modeling and observational studies have shown changes in the width and precipitation intensity of this region of the Hadley circulation. The goal of this study is to determine how well existing atmospheric reanalyses capture characteristics of the Pacific ITCZ over the past 35 years using an automated identification algorithm which includes the ITCZ center, width, boundaries, and precipitation intensity within the convergence zone. ECMWF Reanalysis Interim (ERA-Interim) and the second edition of the Modern-Era Retrospective analysis for Research and Applications (MERRA-2) are compared against results obtained using the Global Precipitation Climatology Project (GPCP) observations in Wodzicki and Rapp. The reanalyses are found to be capable of reproducing similar ITCZ characteristics as GPCP, but not without disagreements. The ERA-Interim reanalysis produces a wider ITCZ on average than either MERRA-2 or GPCP, particularly on the southern extent. Analysis of the dynamic and thermodynamics of the two reanalyses shows that ERA-Interim produces a broad region of ascent that does not sufficiently separate the ITCZ and Southern Pacific Convergence Zone (SPCZ) regions in the central Pacific. This lack of separation results in the automated method identifying an ITCZ that extends further south than what is shown by GPCP and MERRA-2. Despite these differences, long-term reanalysis-produced ITCZ trends are similar to observational narrowing and intensification trends, but with varying magnitudes.

CONTRIBUTORS AND FUNDING SOURCES

The automated algorithm used in this study was developed by Kyle Wodzicki and Anita D. Rapp. The members of the thesis committee Anita D. Rapp, Christopher Nowotarski, and Andrew Klein provided valuable guidance and insight throughout the research and writing process.

This graduate study was funded by NASA grant NNX13AG91G.

NOMENCLATURE

AGCM	Atmospheric general circulation model
AR5	IPCC Fifth Assessment Report
CMAP	CPC Merged Analysis of Precipitation
CMIP5	Coupled Model Intercomparison Project Phase 5
CPC	Climate Prediction Center
CPAC	Central Pacific Ocean
CPCU	CPC Unified Gauge-Based Analysis of Global Daily Precipitation
EPAC	Eastern Pacific Ocean
ECMWF	European Centre for Medium-Range Weather Forecasts
ERA-40	ECMWF 40-year Reanalysis
ERA-Interim	ECMWF Reanalysis Interim
GCM	General circulation model
GEOS-5	Goddard Earth Observing System Model, version 5
GPCP	Global Precipitation Climatology Project, version 2.2
HRC	Highly reflective cloud
IFS-Cy31r2	Integrated Forecast System, cycle 31r2
IPCC	Intergovernmental Panel on Climate Change
ITCZ	Intertropical Convergence Zone
MERRA	Modern Era Retrospective-Analysis for Research
MERRA-2	Second Edition of the MERRA Reanalysis

NASA	National Aeronautics and Space Administration
NOAA	National Oceanic and Atmospheric Administration
Omega	Vertical Pressure Velocity
RR	Rain rate
SPCZ	South Pacific Convergence Zone
SSM/I	Special Sensor Microwave/Imager
TMI	TRMM Microwave Imager
TRMM	Tropical Rainfall Measuring Mission

TABLE OF CONTENTS

LIST OF FIGURES

LIST OF TABLES

1. INTRODUCTION

The Intertropical Convergence Zone (ITCZ) is a semi-permanent feature of the tropical atmosphere. This region is characterized by the lower atmospheric convergence of northeasterly and southeasterly trade winds over the Pacific Ocean (Bjerknes et al. 1969). This convergence of winds forms a narrow band that produces consistent convection and heavy precipitation (Estoque and Douglas 1978; Frank 1983). Figure 1.1 shows a time-averaged contour map of the Global Precipitation Climatology Project (GPCP) [Adler et al., 2003; Huffman et al., 2009] rain rate data over the Pacific Ocean. A clearly defined band of heavy rain emerges between 0° - 15° N that spans nearly the full length of the Pacific; the climatological mean ITCZ center is near 8° N (Gruber 1972; Mitchell and Wallace 1992; Waliser and Gautier 1993). A separate, but related, feature is the Southern Pacific Convergence Zone (SPCZ) which is the heavy precipitation region between 0° - 15° S in the western portion of the Pacific.

The ITCZ can also be identified as a broad region of enhanced cloudiness that is only readily apparent beyond a daily time scale (Hubert et al. 1969; Holton et al. 1971) since the ITCZ often produces isolated, disorganized convection (Frank 1983; Wang and Magnusdottier, 2006). On a monthly or yearly scale, the ITCZ generates the consistent precipitation evidenced by Figure 1.1 that is important to the tropical, and global, atmosphere. The large amounts of precipitation produced in this region make it a primary mechanism for the transfer of latent heat and energy to the higher latitudes via the global scale Hadley circulation.

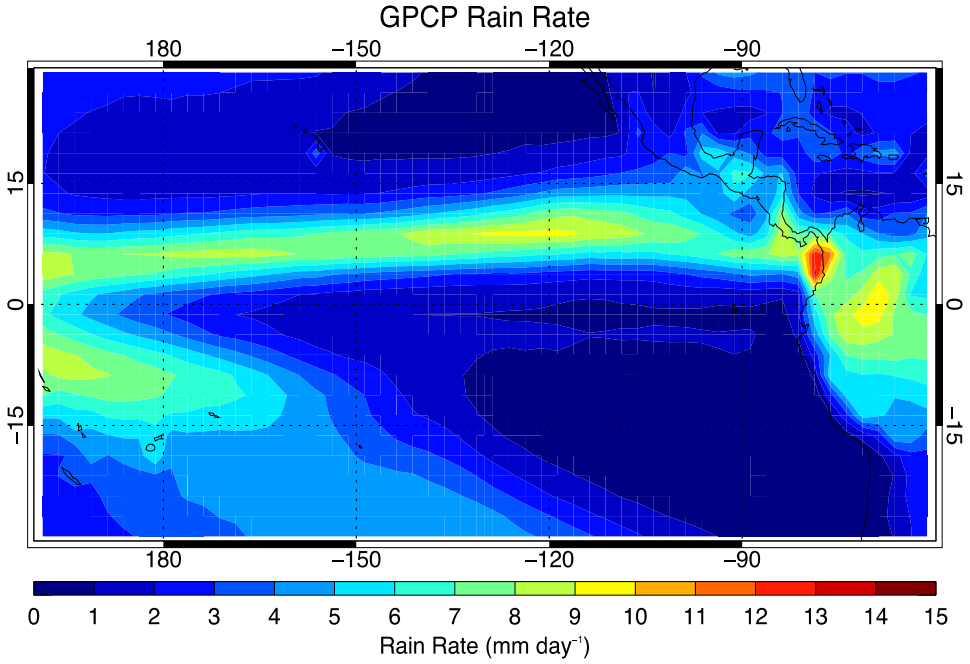

Figure 1.1: GPCP rain rate climatology over the Pacific Ocean from 1980 – 2014.

Early research implied that ITCZ convection is a main driver of the Hadley circulation (Fletcher 1945; Riehl and Malkus 1958; Asnani 1968). The warmer tropics constitute the Hadley Cell's ascending branch by producing convection and spreading warm, moist air poleward in the upper atmosphere (Webster 2004). The subsiding branch falls between 20° - 30° in both hemispheres and the low level divergence produced provides an equatorward return of cooler, drier air. Some of the heaviest rainfall in the world is located within the ascending branch of the Hadley Cell and some of the driest near the descending branches (Lu et al. 2007; Seidel et al. 2008; Stachnik and Schumacher 2011). Given that the ITCZ constitutes the rising branch of the Hadley

Cell in the Pacific, it is critical to understand the drivers behind the ITCZ and any changes that may occur with a changing climate.

Under greenhouse gas warming scenarios, global climate models (GCMs) generally show both a deepening of convection and meridional narrowing of the ITCZ extent while showing a strengthening of the Hadley circulation overall. However, Mitas and Clement (2006) showed that the GCMs have large variability in the strength of the Hadley circulation. The widening of the Hadley circulation in GCMs has been exhaustively studied in a warming climate (Lu et al., 2007; Seidel et al., 2008, Levine and Schneider, 2015); however, Pierrehumbert (1995) noted that the response of the ITCZ width and precipitation intensity had received little notice even though it is vitally important to the ascending branch of the Hadley Cell.

There is a consensus that a warming climate makes the atmosphere more moist (Houghton et al. 2001). While there are variations in regional response in the tropics, modeling studies by Chou and Neelin (2004) showed that convective zones in the tropics are expected to narrow with warming due to drying of the subtropical air. This air is then advected equatorward and produces narrowing convective regions and a reduction in precipitation on the margins of the convective zones. In a similar study, Neggers et al. (2007) suggested that a reduction in subtropical moistening by shallow clouds leads to a narrowing of the ITCZ and increases precipitation intensity. Other recent studies have shown the ITCZ narrows in future warming GCM scenarios (Huang et al., 2013; Lau and Kim, 2015). This conclusion was also reached while using rainfall observations and satellite data (Wodzicki and Rapp, 2016). Using Global Precipitation Climatology

Project (GPCP) [Adler et al., 2003; Huffman et al., 2009] and Tropical Rainfall Measuring Mission (TRMM) [Kummerow et. al., 1998] data, they found both ITCZ narrowing and rain rate intensification trends in the Pacific since 1979. The fifth phase of the Coupled Model Intercomparison Project (CMIP5) also showed a near consensus that the ascending branch of the Hadley circulation was both narrowing and intensifying (Taylor et al. 2012; Su et al., 2017). While there seems to be a consensus that the ITCZ is narrowing and convection is intensifying, the methods used to identify and quantify the ITCZ are not consistent among the aforementioned studies.

There are a wide variety of definitions for the ITCZ location and its boundaries. One of the earliest studies done by Waliser and Gautier (1993) made use of the highly reflective cloud (HRC) data set which is a combination of visible and infrared satellite imagery (Garcia 1985). The ITCZ was simply defined where a HRC was present in a set amount of days per month. However, this particular HRC data set was limited to data from 1971-1987. This study contributed valuable information on the location and seasonal migration of the ITCZ, but the precipitation intensity could not be inferred and the short data set could not be used to study long-term changes.

Bain et al. (2011) found the same seasonal and migratory patterns of the ITCZ by using a statistical approach combining three satellite observations: infrared brightness temperature, visible reflectance, and total precipitable water. The study was also temporally limited because all three data sets were available for a total of 13 years from 1995-2008, but the infrared had a temporal range from 1980-2009. Their study, like

Waliser and Gautier (1993), was also for a limited time period and only used observations.

Given that the use of clouds and temporal range were issues in early studies, Berry and Reeder (2014) turned to reanalyses. They used daily dynamic and thermodynamic fields from the European Centre for Medium-Range Weather Forecasts (ECMWF) Reanalysis Interim (ERA-Interim) [Dee et al., 2011] from 1979-present. Berry and Reeder (2014) used masks with various thresholds to identify an ITCZ presence by using a seven-day running mean from daily scale data. Wodzicki and Rapp (2016) used a modified version of the Berry and Reeder (2014) algorithm. In lieu of the seven-day mean used by Berry and Reeder, they used monthly mean dynamic and thermodynamic variables obtained from ERA-Interim and both GPCP and TRMM rain rate observations to identify long-term ITCZ variability. Using ERA-Interim and satellite observed rain rates, Wodzicki and Rapp (2016) found significant narrowing and rain rate intensification for the ITCZ. They used the reanalysis to identify long convergent regions and observational rain rates to capture ITCZ width and found general consistency between the region of heaviest observed precipitation and reanalysis convergence. However, the consistency between observations and reanalysis precipitation was not tested and it remains unclear whether reanalyses capture the width of the ITCZ precipitation zone and the precipitation intensity. Here we examine the ERA-Interim and the second edition of the Modern-Era Retrospective analysis for Research and Applications (MERRA-2) produced by the National Aeronautics and Space Administration (NASA) [Gelaro et al., 2017].

The precursors to the two reanalyses used in this study were found to have significant issues in precipitation. ERA-40, for instance, overestimated rainfall greatly over tropical oceans due to their humidity analysis and infrared radiance schemes (Uppala et al. 2005). Sun et al. (2018) found that the first edition of MERRA also overestimated extreme precipitation in the Indian Ocean, the Pacific Ocean and western Atlantic Ocean. Both ECMWF and NASA put significant work into improving their hydrology schemes for the newer reanalyses.

The ERA-Interim reanalysis now uses a completely automated scheme to adjust for biases found in radiance observations; they also improved boundary layer cloud physics and adjusted atmospheric stability which has resulted in less overall precipitation (Dee et al. 2011). A study of monsoon regions implied that ERA-Interim was the best overall reanalysis for climatological and interannual precipitation (Lin et al. 2014). The study does, however, concede there is an obvious overestimation in rain rates between the range of 10-20 mm/day. The ITCZ frequently produces rain rates in this range, but the tropical atmospheric divergence appears to be realistic when compared to evaporation and precipitation estimates (Brown and Kummerow, 2014). Similarly, the MERRA-2 reanalysis made significant changes and improvements to their precipitation scheme.

The main deviation in the MERRA-2 hydrological cycle from MERRA is the enforcement of a constraint between evaporation and precipitation that help balance the total atmospheric water mass storage (Takacs et al. 2016). This has led to significant improvements, especially over ocean surfaces. The MERRA-2 hydrological cycle

overestimates surface evaporation over the ocean, but the precipitation is close to observed (Rodell et al. 2015). Over land, the precipitation suffers, but this is generally attributed to rainfall over high elevations such as the Andes mountains (Bosilovich et al., 2015). Bosilovich et al. (2017) performed an exhaustive analysis of the MERRA-2 hydrological cycle and its differences to MERRA. The updated reanalysis still produces excessive rainfall in the warm pool region in the western Pacific and the eastern Pacific remains close to the observational GPCP except in the areas directly adjacent to the coast of the Americas. Although the reanalyses have made improvements, it is important to test how they handle the high precipitation in the ITCZ region.

This study attempts to apply the fully automated algorithm that identifies the center of the ITCZ and the boundaries used by Wodzicki and Rapp (2016) on the two discussed reanalyses: ERA-Interim and MERRA-2. The ITCZ extent and rain rate intensity will also be studied. The ITCZ center is found by modifying the Berry and Reeder (2014) method to work for a monthly time scale and the boundaries are then identified using rain rate fields after the ITCZ center is established. Beyond identifying and studying changes in the ITCZ, this study also aims to identify drivers behind differences in these reanalyses' physics that affect the ITCZ and its long-term trends.

2. DATA AND METHODS

Numerous studies have shown that the region of heavy precipitation corresponding with the Intertropical Convergence Zone (ITCZ) becomes both narrower and more intense under greenhouse gas forcing scenarios (Huang et al., 2013; Lau and Kim, 2015; Su et al., 2017). This research aims to compare reanalysis data to the narrowing and intensification trends found in observational and modeling research. A reanalysis is systematic approach of modeling the atmosphere which produces data sets that blend observations within an unchanging data assimilation scheme. Two reanalyses are used to analyze the ITCZ: the European Centre for Medium-Range Forecasts (ECMWF) European Reanalysis (ERA-Interim) [Dee et al., 2011] and the second edition of the Modern-Era Retrospective analysis for Research and Applications (MERRA-2) produced by the National Aeronautics and Space Administration (NASA) [Gelaro et al., 2017]. The two reanalyses are widely used in the literature though they are two very different products.

The MERRA-2 reanalysis uses the Goddard Earth Observing System Model version 5 (GEOS-5) while the ERA-Interim data set uses a fixed version of the numerical weather prediction system (IFS-Cy31r2). MERRA-2 blends two observation data sets collected by the NOAA Climate Prediction Center (CPC): the CPC Unified Gauge-Based Analysis of Global Daily Precipitation (CPCU) product and the CPC Merged Analysis of Precipitation (CMAP) product (Reichle et al., 2017). The study considered using Global Precipitation Climatology Project (GPCP) Version 2.2 data, but

the MERRA-2 reanalysis requires data that is updated operationally with a latency less than about one week which GPCP does not do. Reichle et al. (2017) notes that "GPCPv2.2, CMAP, and, to a lesser extent, CPCU data share a substantial portion of their raw gauge and/or satellite radiance inputs" so GPCPv2.2 is not a completely independent reference for the correction of the MERRA-2 precipitation scheme. ERA-Interim assimilates clear-sky radiances from the Special Sensor Microwave Imager (SSM/I) (Conner and Petty, 1998). This assimilation system also makes use of the rain-affected SSM/I radiances which were not present in the ERA-40 reanalysis (Dee et al., 2011). These two data sets are compared against the Global Precipitation Climatology Project (GPCP) [Adler et al., 2003; Huffman et al., 2009]. GPCP merges data collected from a variety of sources including rain gauges, satellites and sounding observations dating back to 1979. Using satellite estimates to fill in the spatial detail between land, GPCP is the most complete global precipitation data set.

For this analysis we are using the method developed by Wodzicki and Rapp (2016), who found the center of the ITCZ using U- and V-wind components, relative humidity, and temperature; the northern and southern boundaries are defined by rain rate. The region of focus is in the Pacific between 45°S - 45°N and 160°E - 160°W (central Pacific) and 140°W - 100°W (east Pacific). The time range studied is January 1980 to December 2014. For a consistent comparison to GPCP, all rain rates are used at 2.5° x 2.5°. Wodzicki and Rapp (2016) originally used the ERA-Interim 1.5° x 1.5° data set for the ITCZ center identification which is also used here for MERRA-2. All data,

Variable	Levels Required (hPa)	1.5° x 1.5°
U component of wind	1000-850	1.5° x 1.5°
V component of wind	1000-850	1.5° x 1.5°
Temperature	850	1.5° x 1.5°
Relative Humidity	850	1.5° x 1.5°
Rain Rate	N/A	2.5° x 2.5°

Table 2.1 Variables used in ITCZ identification. All variables were collected on a six-hour time step. The native resolution for ERA-Interim is ~0.7° x ~0.7° and MERRA-2 is 0.5° x 0.625°

found in Table 2.1, were either downloaded pre-gridded to match or interpolated to fit the GPCP latitude/longitude scheme.

2.1 Method for ITCZ Identification

The first step in testing how well the reanalyses capture ITCZ characteristics is to identify the ITCZ center. Wodzicki and Rapp (2016) modified a version of Barry and Reeder (2014), which originally used seven-day means for daily ITCZ identification. For this research, monthly mean analysis is deemed sufficient given our interest in long-term variability. The first step in identifying the ITCZ center is calculating the layer mean divergence from 1000-850hPa using 5-point smoothed U- and V-wind components. The gradient of divergence is then calculated and locations where the gradient of divergence equals zero are taken as the first guess for the ITCZ center. While this method does place a line in the convergence zone we expect near 15°N as noted in Figures 2.1(a) and

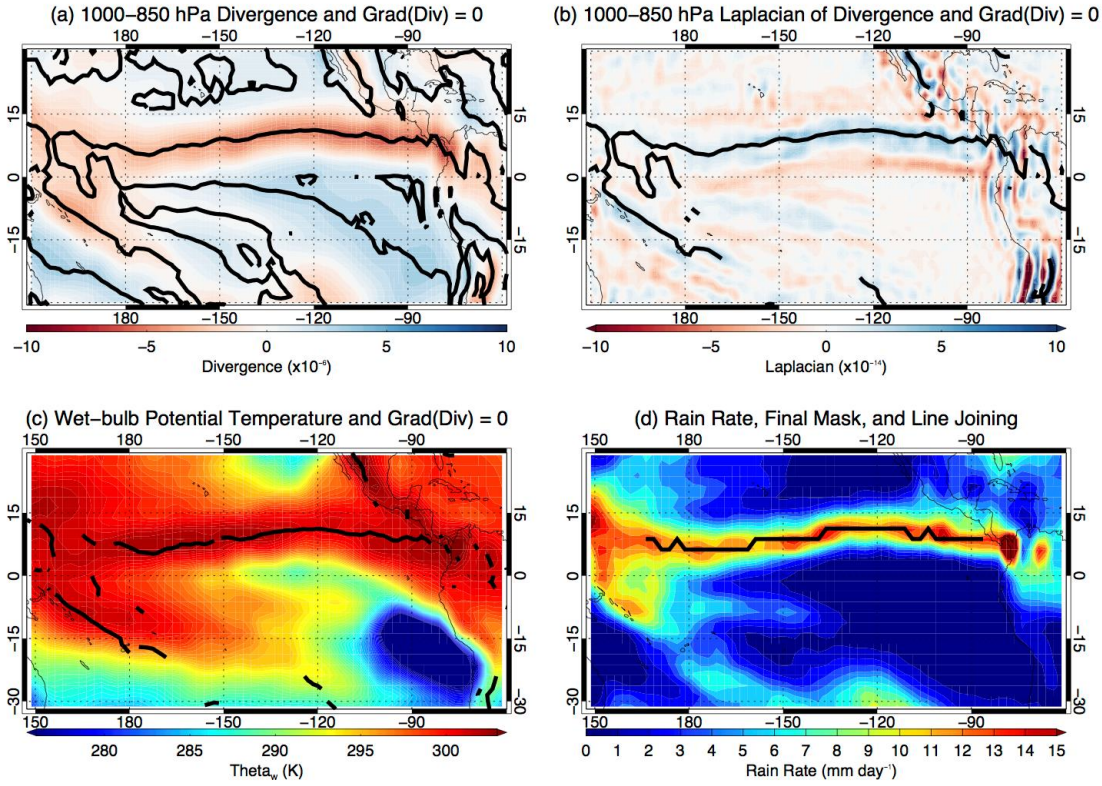

Figure 2.1: Reproduction of the ITCZ identification method outlined by Wodzicki and Rapp [2016] (similar to their Figure 1), for August 2004 using ERA-Interim variables. (a) Divergence and gradient of divergence equal to zero (line); (b) Laplacian of divergence and gradient of divergence equal to zero after divergence mask has been applied (line); (c) θ_w and gradient of divergence equal to zero with both divergence and Laplacian of divergence masks applied (line); (d) ERA-Interim rain rate and gradient of divergence equal to zero after the application of all masks and final line joining.

2.2(a), there are many other locations where the gradient of divergence equals zero which need to be removed. Removing false ITCZ locations uses three additional masks. The first removes any identifications where the divergence is above a threshold of -1 x $10^{-6}\ s^{-1}$. This is done to isolate any areas of convergence as the most likely candidates for the center of convergence in the ITCZ. In Figures 2.1(b) and 2.2(b), the application of this mask removes most misidentifications south of the equator and north of 15°N.

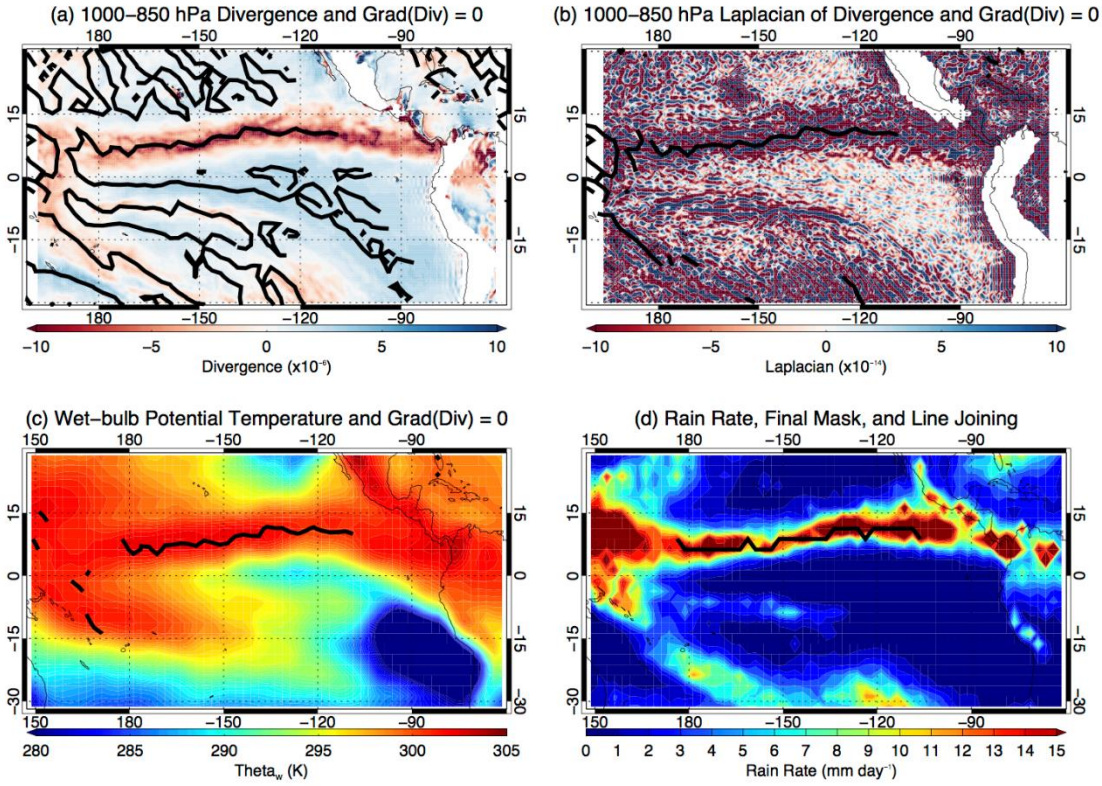

Figure 2.2: Reproduction of the ITCZ identification method outlined by Wodzicki and Rapp [2016] (similar to their Figure 1), for August 2004 using MERRA-2 variables. (a) Divergence and gradient of divergence equal to zero (line); (b) Laplacian of divergence and gradient of divergence equal to zero after divergence mask has been applied (line); (c) θ_w and gradient of divergence equal to zero with both divergence and Laplacian of divergence masks applied (line); (d) MERRA-2 rain rate and gradient of divergence equal to zero after the application of all masks and final line joining.

The second mask uses the Laplacian of the layer mean divergence to filter out any inflection points that aren't divergence maxima or minima but still cause the gradient of divergence to equal zero. From Wodzicki and Rapp (2016), the Laplacian of divergence is also the divergence of the gradient of divergence so locations of maximum Laplacian of divergence will be collocated with absolute divergence minima. Any ITCZ locations

with Laplacian of divergence values below the threshold of 4 x 10^{-18} $m^{-2}s^{-1}$ are removed. Figure 2.1(c) shows the results of this mask which has removed most of the false identifications.

The third mask uses the temperature and relative humidity fields at 850 hPa to calculate the wetbulb temperature, which is used to distinguish the tropics and the extratropics. Any ITCZ identifications that fall below a wetbulb potential temperature threshold of 297 K are removed, which implies that the only remaining potential ITCZ locations are in the tropics. Since the ITCZ center often is disconnected, a line joining process similar to Barry and Reeder (2014) is applied. This process connects any ITCZ identifications within a given latitude and longitude of each other to create a single line of values defined as the ITCZ center. The line joining process also fixes the final center line onto the GPCP resolution of 2.5° x 2.5° which is why the final result in Figures 2.1(d) 2.2(d) are not as smooth as in Figures 2.1(c) and 2.2(c).

2.2 Identifying ITCZ Boundaries

There are a variety of definitions for the ITCZ boundaries such as the total area of ascent in the Pacific or the amount of high clouds (< 440 hPa) in a given length of time (Byrne and Schneider, 2016; Su et al., 2017), but the use of GPCP provides a real-world observational comparison. The variety of variables produced by reanalyses open up the possibility of using different boundary definitions, but using the same method as Wodzicki and Rapp (2016) provides a consistent comparison to fields that can actually be observed.

The ITCZ boundaries are established after the center is identified. From the ITCZ center, iterations north and south are made over the rain rate fields until the values fall below a threshold. Wodzicki and Rapp (2016) found this threshold by comparing ITCZ widths produced by different resolutions of TRMM and GPCP data. Different thresholds and smoothing were tested on the rain rate data to see which combination would produce both the highest correlation between ITCZ widths using both data sets and a slope closest to one; a 2.5 mm/day threshold and a 5-point smoother produced the most consistent results between different observational datasets. For the identification scheme, the grid box immediately poleward with a value below the 2.5 mm/day threshold is defined as the ITCZ boundary. This is performed over every longitude value for which an ITCZ center is identified. The value of the northern and southern boundaries are in degrees latitude and are forced onto the same grid as the rain rate field which is 2.5° x 2.5°. Doing this creates noise on the boundaries that is an artifact of the method, but monthly averages are taken across the full Pacific, EPAC, and CPAC regions so it is mostly filtered out. Figure 2.3 shows the three different rain rate fields with their respective ITCZ centers and boundaries for the month of August 2004. The northern and southern ITCZ widths (km) are then calculated as the distances between the ITCZ center and the boundaries. The total width is simply the sum of these two values. These ITCZ characteristics (e.g. ITCZ center, width, boundary locations, rain rate) are then compared in several different ways including scatterplots, time series, and seasonally both between the reanalyses and to the observational ITCZ characteristics.

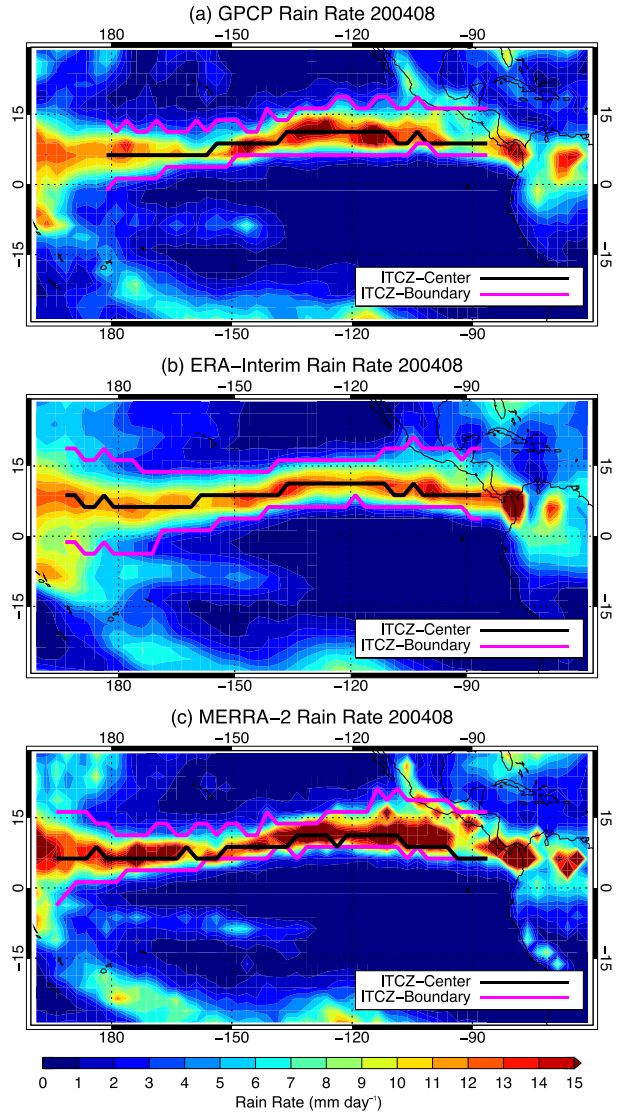

Figure 2.3: Example of ITCZ identifications from the three data sets for August 2004. (a) GPCP rain rate with ITCZ center (black) and ITCZ boundaries (magenta); (b) ERA-Interim rain rate with ITCZ center (black) and ITCZ boundaries (magenta); (a) MERRA-2 rain rate with ITCZ center (black) and ITCZ boundaries (magenta).

2.3 Comparison of Reanalysis Physics

Comparisons between the reanalyses are made using the remaining variable fields such as vertical pressure velocity (ω), temperature, and specific humidity. These particular variable fields give a glimpse into the physics behind the ITCZ in each reanalysis. Divergence and ω present the dynamic nature of the ITCZ as it relates to overall circulation, while temperature, specific humidity and relative humidity show how the ITCZ operates thermodynamically. Vertical climatologies of the dynamic and thermodynamic variable fields are constructed by averaging meridionally along each latitude band between the boundaries of the central and eastern Pacific, respectively. Since ERA-Interim and MERRA-2 use slightly different pressure level schemes, only the levels the two reanalyses have in common are considered. They range from 1000-50hPa at intervals of 25hPa between 1000-800hPa and then by 50hPa afterwards for a total of 24 pressure levels. The variables are then time averaged and latitude vs. pressure composites are produced of each field and then of the difference between the reanalyses are computed. ERA-Interim is used as the baseline for comparison so the difference plots are always MERRA-2 subtracted from ERA-Interim. Average locations from the ITCZ boundaries are superimposed onto these composites so that the differences in the physics near the ITCZ can be determined.

2.4 Testing the Methodology

The ITCZ boundaries are dependent entirely on rain rate fields dropping beneath a given threshold. The decision to use rain rates as the ITCZ boundary definition was made in order to compare it to the observational GPCP. Numerous studies have been

done using other definitions of the ITCZ boundaries, it was worth exploring if any others would have produced more realistic results for any given month. A random month is chosen to illustrate different methodologies: March 2010.

The study from Byrne and Schneider (2016) used the ω values at the 500 hPa pressure level (ω_{500}) to define the ITCZ. Their method simply identified the center of convergence and the boundaries were where the ω_{500} changed from negative to positive ω, or from upward motion to downward motion. Another method using the same line of thought defines the ITCZ as where there is widespread layer mean convergence, or that the ITCZ boundaries are where the wind fields show a change in divergence. While there are other methods such as Dias and Pauluis (2011) definition based on brightness temperature, these two ITCZ boundary definitions are chosen since they represent the physical processes that drive the ITCZ (convergence and upward motion). It is important to note that these methods were tested, but ultimately not used because they cannot be directly compared to GPCP like the rain rate threshold method.

Figure 2.4 displays the three rain rate contours obtained from each data set for March 2010 with their respective ITCZ centers and boundaries overlaid. In ERA-Interim, the algorithm produced a straight line from the last place the ITCZ boundary was below the threshold to the western edge of the ITCZ. The boundaries are found only by iterating from the center ITCZ so the boundaries are never shorter longitudinally than the center and a boundary must exist. The straight line in the central Pacific region is an attempt by the algorithm to separate the SPCZ and ITCZ boundaries. Clearly the

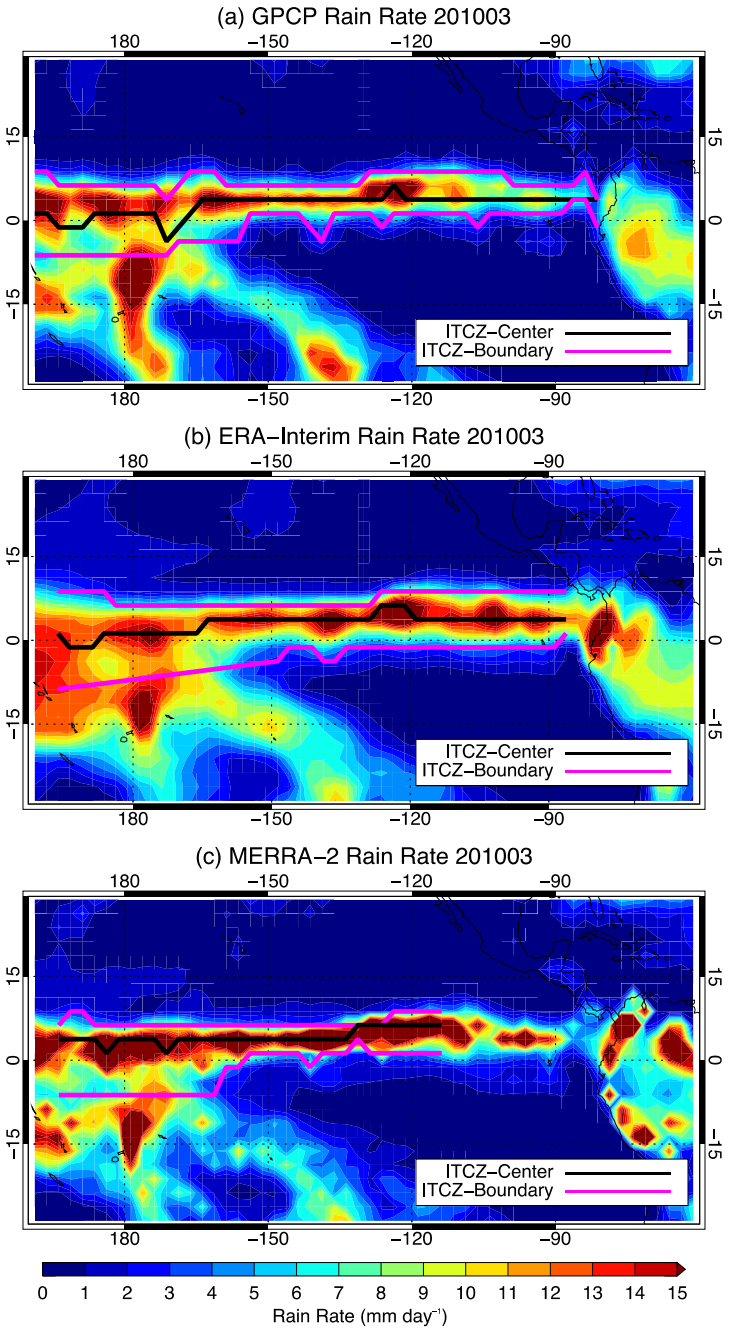

Figure 2.4: Same as in Figure 2.3, but for March of 2010.

threshold used in this study breaks down when the rain rates between the SPCZ and ITCZ are not separated.

The top panel in Figure 2.5 shows the ERA-Interim rain rate with the ITCZ boundaries found by the rain rate threshold in magenta and the contour locations where the layer mean (1000-850 hPa) divergence equals zero. The plot directly beneath displays the same information except the black lines represent where ω_{500} equals zero. Using divergence as a proxy for ITCZ boundaries yields differing results for the two boundaries. The process would work nearly as well as rain rate on the northern edge of the ITCZ, but it would be farther north at all points. The southern boundary is also too wide, especially in the eastern half of the Pacific. In the west, the divergence would not capture the ITCZ correctly. While there is a line where the divergence would place a correct looking boundary in the central Pacific, there is more than a 5° difference between that and the line in the eastern Pacific. In this case automation would likely fail or the ITCZ would have to be truncated at 160°W.

The ω_{500} method also contains mixed results. The northern boundary agrees exceptionally well with the rain rate threshold method, but the southern boundary does not. As in the divergence test, the eastern portion of the Pacific does well. The eastern ITCZ placed by ω_{500} would actually agree very well with GPCP which is slightly narrower than the ERA-Interim ITCZ. In the central Pacific, the ω_{500} equals zero line would curve south below 30°S around the SPCZ. Using either of these methods would result in difficulty estimating the location of the southern ITCZ in the central Pacific. Each automated method is subject to breakdowns for different situations; however

dynamic thresholds only do not appear to be an improved method so the rest of the analysis will use the precipitation fields that can be compared to observations.

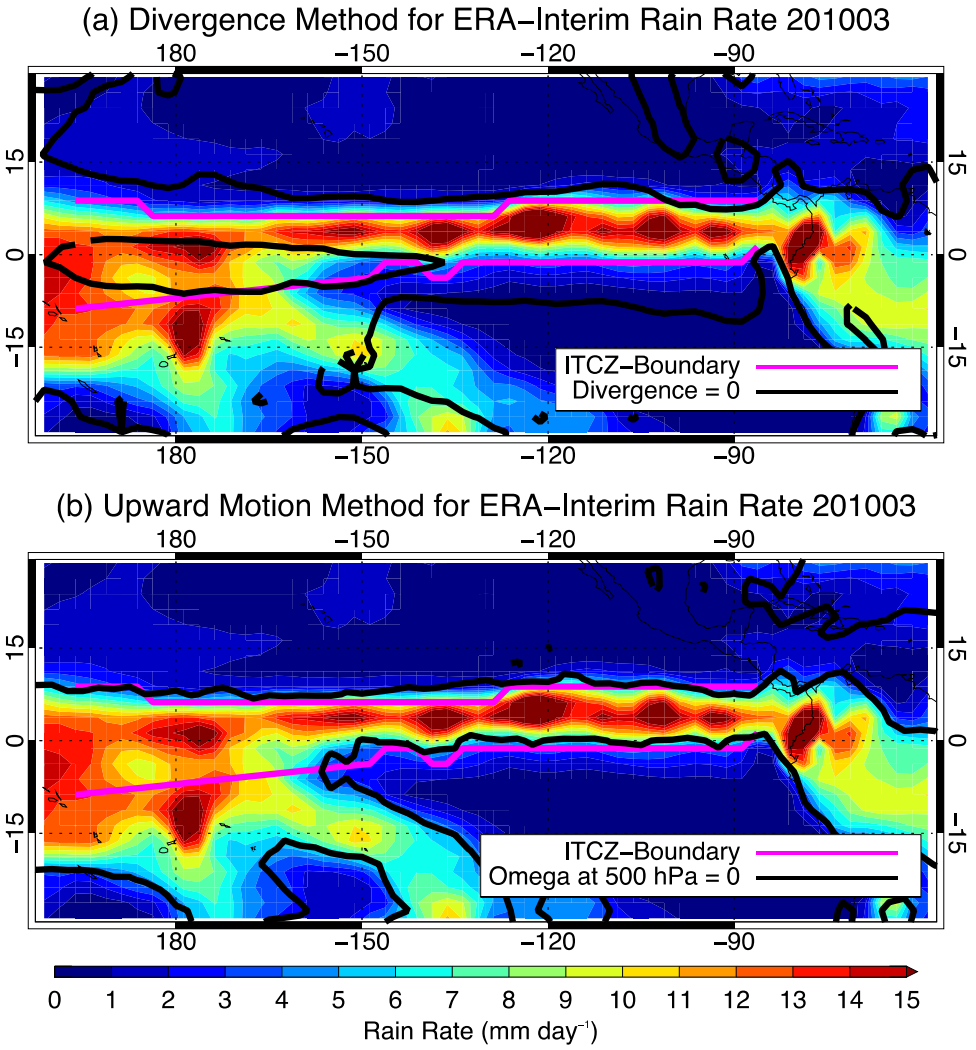

Figure 2.5: (a) Identifying ITCZ boundaries by finding where the 1000-850 hPa layer mean divergence and (b) vertical pressure velocity at 500 hPa equal zero (black); results are compared against the rain rate threshold methodology (magenta).

3. RESULTS

The ITCZ center, ITCZ boundary and rain rate climatologies are averaged over the full longitudinal extent of the ITCZ for each month. Several comparisons such as ITCZ location, latitudinal extent and rain rate intensity are broken into eastern and central Pacific (hereafter EPAC and CPAC, respectively) regions for easier comparisons to previous studies [e.g., Waliser and Gautier, 1993; Zhou et al., 2011; Wodzicki and Rapp, 2016].

3.1 ITCZ Location and Width

Wodzicki and Rapp (2016) found consistency between the ERA-Interim ITCZ center and heavy precipitation in GPCP. Here the consistency of ITCZ location is compared against GPCP with reanalysis derived ITCZ characteristics. Since our definition of the ITCZ extent is simply the distance from the ITCZ center to an ITCZ boundary, it is first important to analyze ITCZ centers produced by the two reanalyses. Figure 3.1 shows the comparison of the average ITCZ center location found between the two data sets. The correlation is high and the two match very well except when the ITCZ is furthest south. The results shown by Figure 3.1 imply a good, but not perfect, agreement between the divergence fields produced by the reanalyses and that any differences in ITCZ characteristics are not due to variations in the placement of the ITCZ center by the two reanalyses.

The location of each ITCZ boundary is averaged over the full length of the ITCZ and then plotted against results obtained from GPCP. The reanalyses'

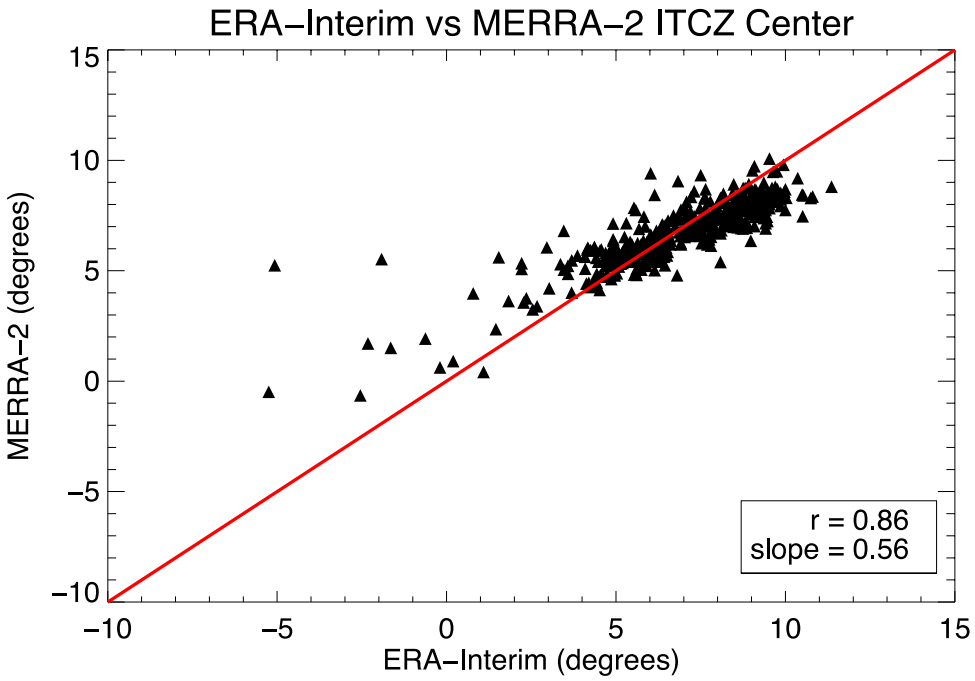

Figure 3.1: Comparison of longitudinally averaged ITCZ center location between the two reanalyses.

northern ITCZ boundaries are compared to the GPCP results in Figure 3.2. Both are highly correlated, but the largest difference is that ERA-Interim places the boundary further north on average than MERRA-2. MERRA-2 also packs the results tightly around the one-to-one line with GPCP results.

The same analysis is done for the southern ITCZ boundary in Figure 3.3. The MERRA-2 southern boundary tends to be closer to the one-to-one line than the ERA-Interim comparison. And, as was the case for the northern boundary, the ERA-Interim places the ITCZ further poleward than GPCP. In both reanalyses, the results are more consistent with GPCP when the ITCZ is further north.

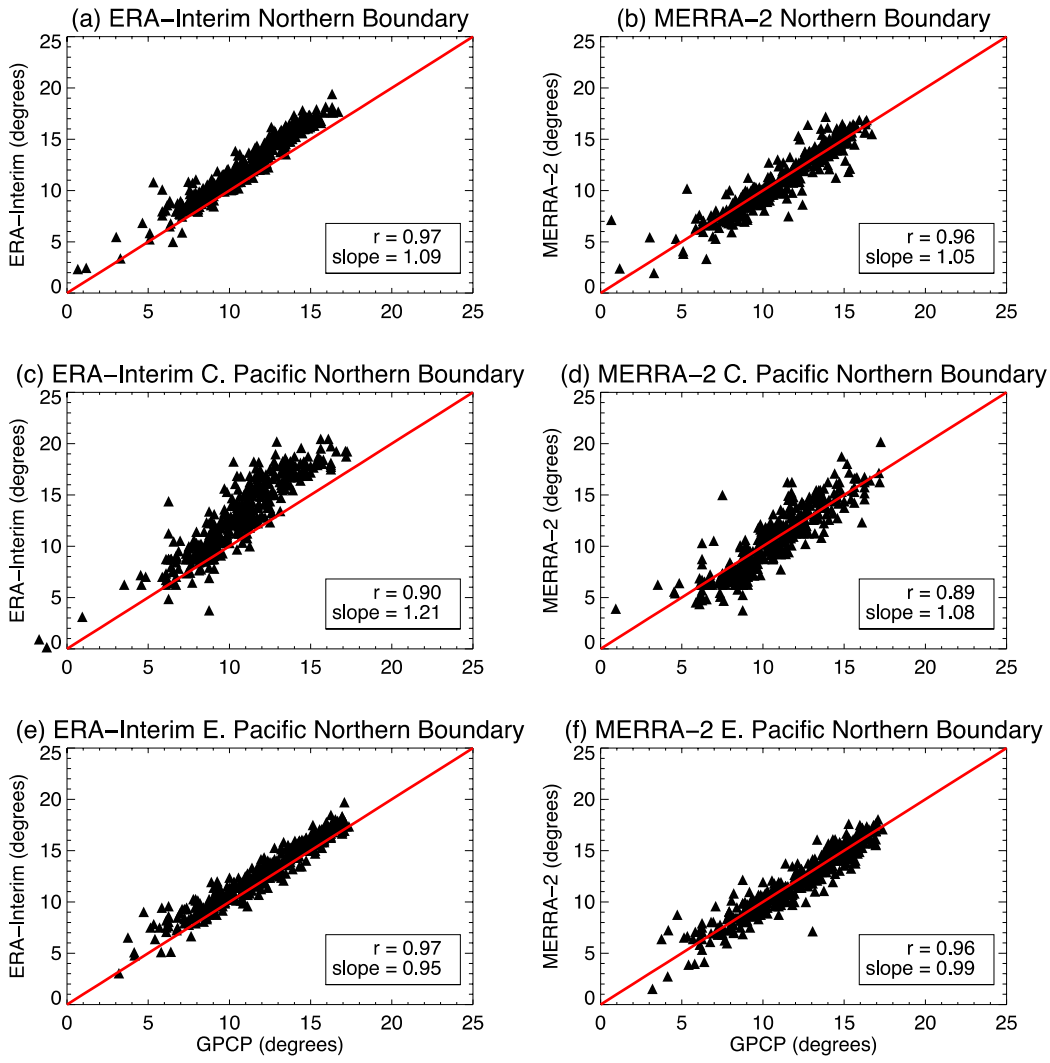

Figure 3.2: (a) and (b) Longitudinally averaged ITCZ northern boundary locations for the two reanalyses over the full Pacific; (c) and (d) same, but for the CPAC region; (e) and (f) same, but for the EPAC region.

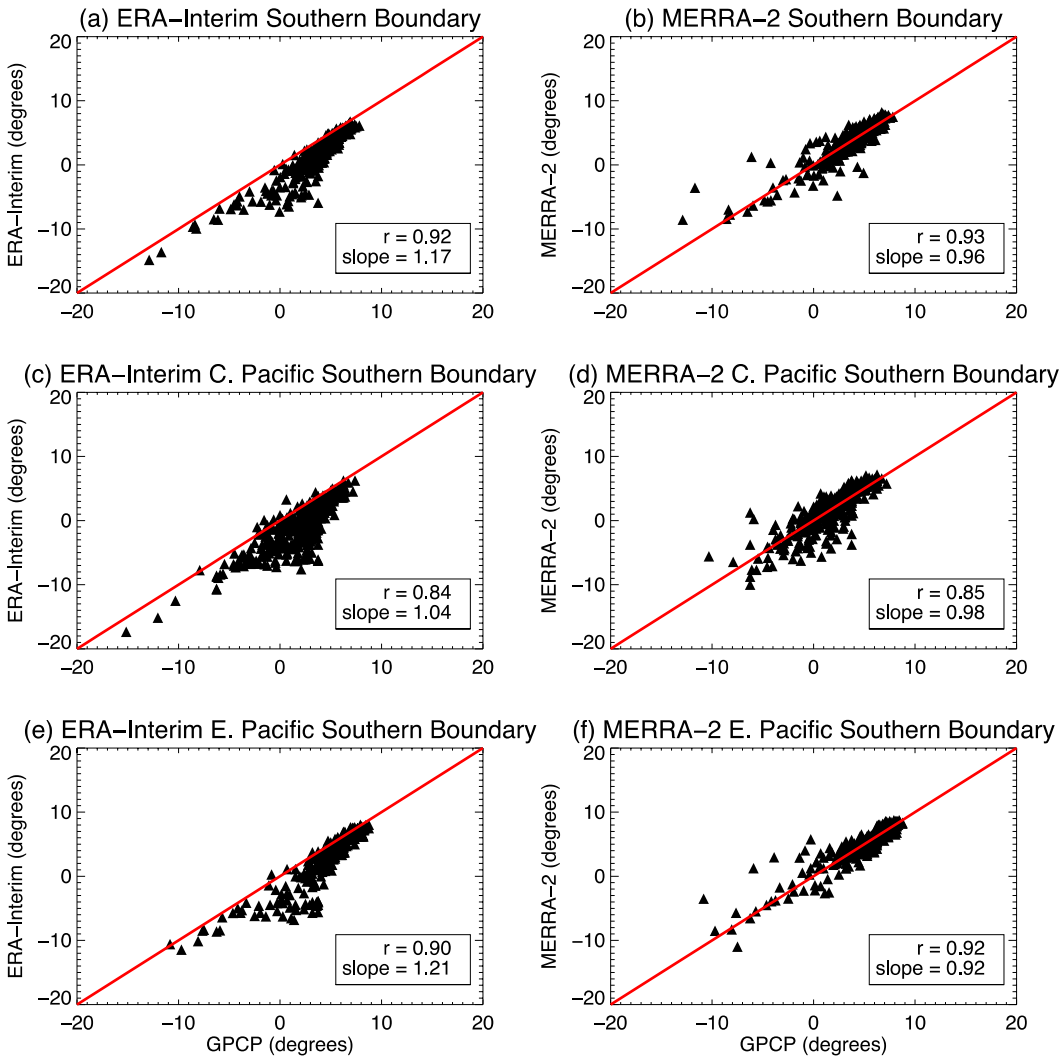

Figure 3.3: Same as in Figure 3.2, but for the southern ITCZ boundary.

		Northern Boundary	Southern Boundary
ERA-Interim	Correlation	0.97	0.92
	Slope	1.09	1.17
	Intercept	0.5	-2.51
MERRA-2	Correlation	0.96	0.93
	Slope	1.05	0.96
	Intercept	-0.55	0.26

Table 3.1: Statistics of the northern and southern ITCZ boundary locations compared to GPCP.

The same scatterplots were made but with the averaging confined to the EPAC and CPAC regions. Figure 3.2(c-f) shows the two reanalyses' results for the northern ITCZ boundary and Figure 3.3(c-f) for the southern boundary. The correlations (Table 3.1) between the reanalyses are still almost identical when divided into regions, but the CPAC slopes are not. There is not much change between the full Pacific and CPAC comparisons between MERRA-2 and GPCP, but the ERA-Interim comparison places the ITCZ too far north, especially when the ITCZ is already furthest north. The EPAC regions in either reanalysis do not exhibit this trait. The same results are found for the southern boundary as well. Both reanalyses produce a larger spread in the results when the ITCZ drifts furthest south. The only difference in this analysis is that MERRA-2 shows a spread in both directions of the one-to-one line while ERA-Interim places its southern boundary almost exclusively further south than GPCP. While it is useful to compare boundary locations, the ITCZ extent from the ITCZ center is also important to consider.

The ITCZ extent across the full longitudinal length of the Pacific, EPAC and CPAC regions is shown in Figure 3.4. The results reveal a significant difference given that ERA-Interim produces an average ITCZ that is wider in all but one month and significantly wider than the GPCP ITCZ. The correlations, slopes and intercepts for these calculations are found in Table 3.2. The MERRA-2 ITCZ shows a spread that has a slope of nearly one and an ITCZ that is of comparable width to GPCP.

		Total Width	Northern Extent	Southern Extent	CPAC	EPAC
ERA-Interim	Correlation	0.76	0.79	0.55	0.67	0.63
	Slope	0.82	0.96	0.79	0.71	0.65
	Intercept	540.63	180.78	301.46	848.5	534.65
MERRA-2	Correlation	0.81	0.7	0.54	0.72	0.81
	Slope	0.94	1.21	0.85	0.91	0.76
	Intercept	60.03	-96.44	56.13	130.11	166.9

Table 3.2: Statistics of the ITCZ widths and northern/southern extents compared to GPCP.

A clear difference is established between the two reanalyses, but it is important to see if this is a regional effect so the width is broken into the CPAC and EPAC regions. In both regions, the ERA-Interim reanalysis produces a wider ITCZ on average than either GPCP or MERRA. Both reanalyses also capture the width of the ITCZ more

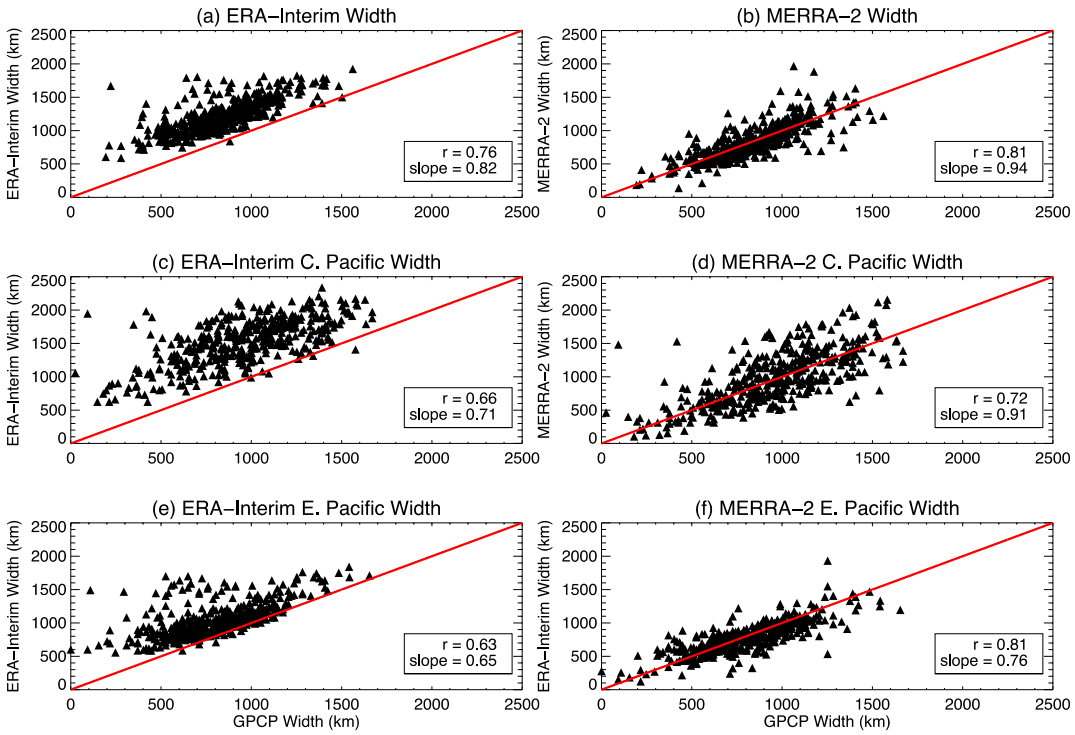

Figure 3.4: (a) and (b) Comparison of longitudinally averaged ITCZ widths between the two reanalyses for the full Pacific; (c) and (d) same, but for the central Pacific; (e) and (f) same, but for the eastern Pacific.

consistently with GPCP in the EPAC region given the scatter of points in the CPAC region. In all comparisons, the MERRA-2 reanalysis produces higher correlations with GPCP than ERA-Interim and a spread of data centered closer to the one-to-one line.

The same analysis was done except for the northern and southern ITCZ widths shown in Figure 3.5. Since the ITCZ extent is found by iterating from the ITCZ center, there are northern and southern portions of the ITCZ width. Both portions of the ERA-Interim ITCZ width extend further poleward than GPCP, and the southern width shows a

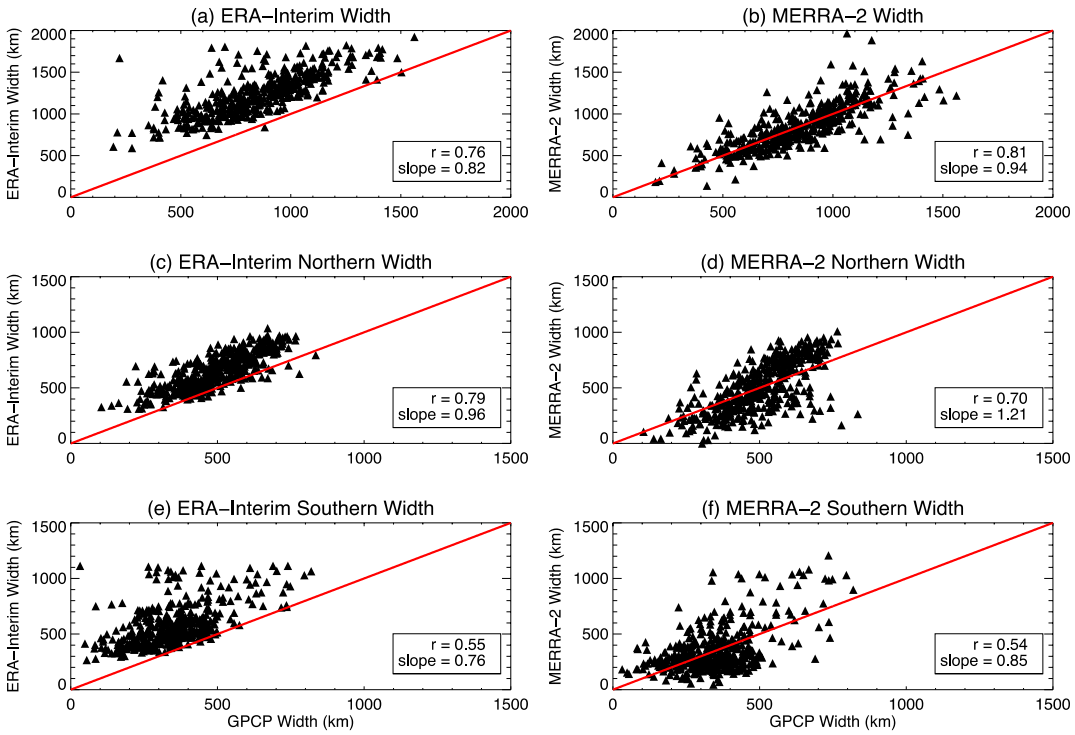

Figure 3.5: (a) and (b) Comparison of longitudinally averaged ITCZ widths between the two reanalyses for the full Pacific; (c) and (d) same, but for the northern ITCZ extent; (e) and (f) same, but for the southern ITCZ extent.

higher spread than the northern portion. This is not the case with MERRA-2 where both portions of the ITCZ show a large spread, but it is significantly worse when the southern boundary of the ITCZ extends furthest south.

The two reanalyses show a distinct difference in ITCZ boundaries and width. The ERA-Interim reanalysis seems to place both ITCZ boundaries further poleward than either GPCP or MERRA-2. While MERRA-2 is consistently closer to the ITCZ locations and width than ERA-Interim, the two reanalyses show similar spread. The

spread tends to be worse in the CPAC and southern portion of the ITCZ width. Since the ITCZ migrates meridionally over the course of a year, it is important to determine if this spread is due to seasonal variations in the ITCZ.

3.2 Monthly and Seasonal ITCZ Trends

The ERA-Interim reanalysis produces an ITCZ that is wider than GPCP or MERRA-2; here we analyze if this is due to seasonal variations in the ITCZ. Figure 3.6 displays the 35-year average ITCZ location for each month. As the individual boundary scatterplots implied, the MERRA-2 reanalysis is in good agreement with the location of the GPCP-obtained ITCZ boundaries. Not only are the boundary locations correct, but the magnitude of the seasonal cycle is nearly identical. The ERA-Interim scatterplots implied a poleward shift that was more apparent in the southern ITCZ boundary. This is also shown in the monthly averages and provides information on which seasons may be causing such a difference. The northern boundary is more northward in every month, but is slightly further in the boreal autumn and winter months. Conversely, the southern boundary in ERA-Interim compares well during these months, but disagrees in the boreal spring months. The magnitude of the seasonal cycle seems to be nearly equal to the MERRA-2 and GPCP results at both boundaries except during these boreal spring months at the southern boundary.

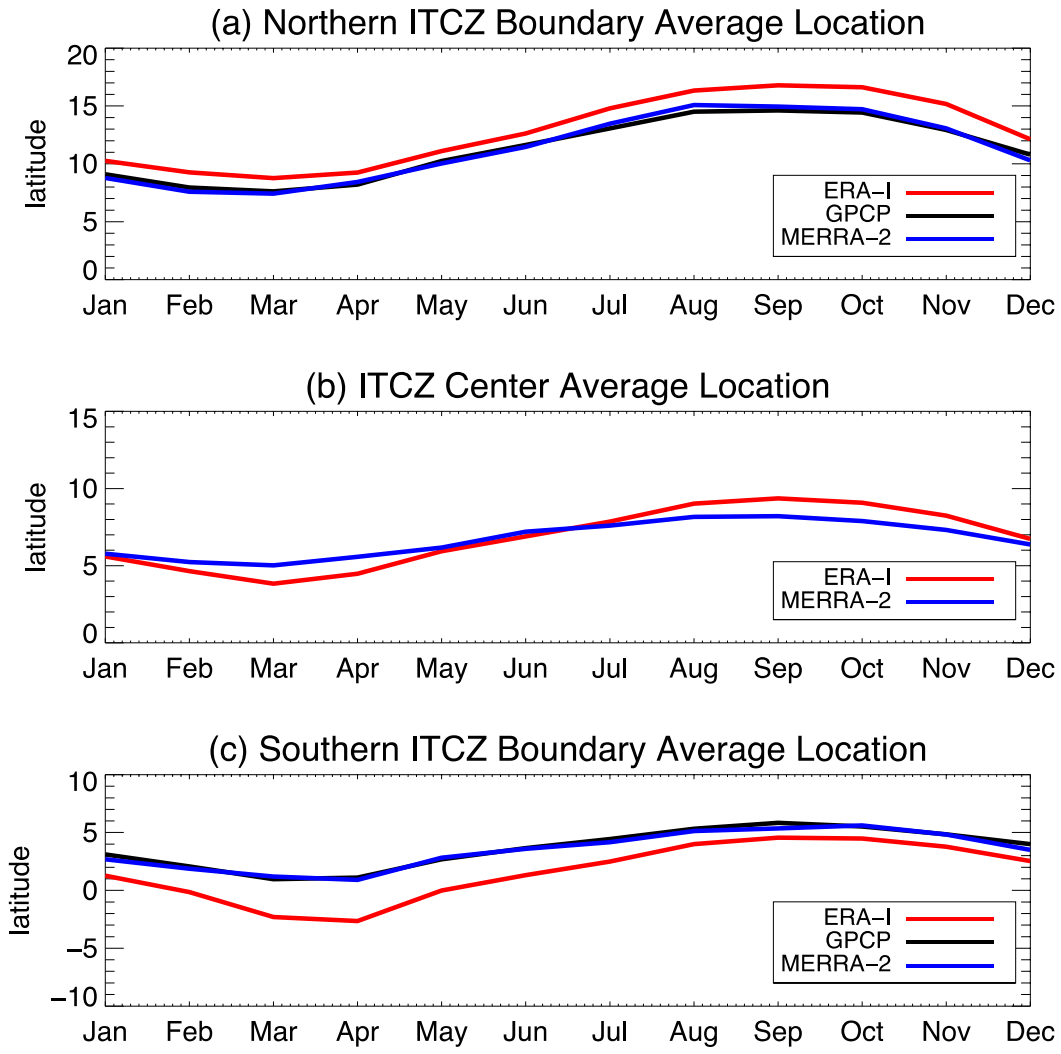

Figure 3.6: Annual cycle of (a) Northern ITCZ boundary; (b) ITCZ center; (c) Southern ITCZ boundary.

The boundaries are then split into seasonal time averages and compared to GPCP. Figures 3.7-10 show these seasonal scatterplots and Tables 3.3-4 show the statistics from these calculations. As expected the MERRA-2 and GPCP comparisons are in good agreement. The ERA-Interim plots further confirm what the annual cycle averaged plots were implying. In the north, there is still a poleward difference compared to MERRA-2, but particularly in the autumn months. While there is a strong correlation, the ERA-Interim boundary is 2°-4° farther north on average during these months. The southern boundary shows nearly the same results but for different seasons. The ERA-Interim autumn and summer months compare well while the winter and spring months show the largest differences, but particularly during the spring where the ITCZ can be 2°-5° degrees further south on average. Figures 3.7-10 show these seasonal scatterplots and Tables 3.3-4 show the statistics from these calculations.

		Spring	Summer	Autumn	Winter
ERA-Interim	Correlation	0.92	0.95	0.89	0.87
	Slope	0.86	1.18	0.85	0.99
	Intercept	2.43	-0.9	4.11	1.31
MERRA-2	Correlation	0.88	0.95	0.85	0.88
	Slope	0.88	1.22	0.96	0.92
	Intercept	1.02	-2.65	0.67	0.37

Table 3.3: Seasonal statistics of the northern ITCZ boundary when compared to GPCP.

		Spring	Summer	Autumn	Winter
ERA-Interim	Correlation	0.88	0.91	0.93	0.91
	Slope	1	1.27	1.03	1.04
	Intercept	-2.998	-2.84	-1.11	-2.1
MERRA-2	Correlation	0.89	0.9	0.91	0.95
	Slope	0.85	1.08	1.04	0.95
	Intercept	0.48	-0.16	0.05	-0.08

Table 3.4: Same as in Table 3.3, but for the southern ITCZ boundary.

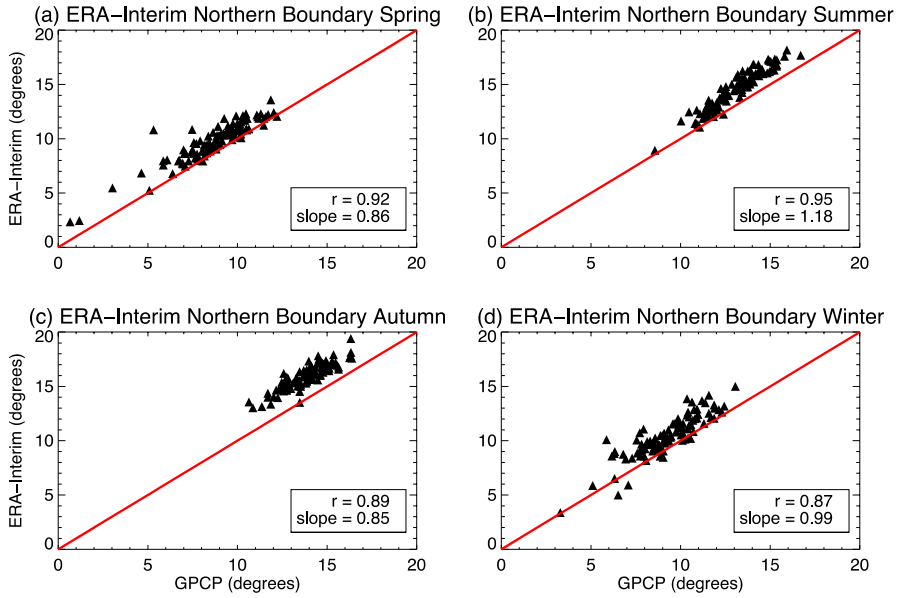

Figure 3.7: Seasonal comparisons of the northern ITCZ boundary location in ERA-Interim to GPCP.

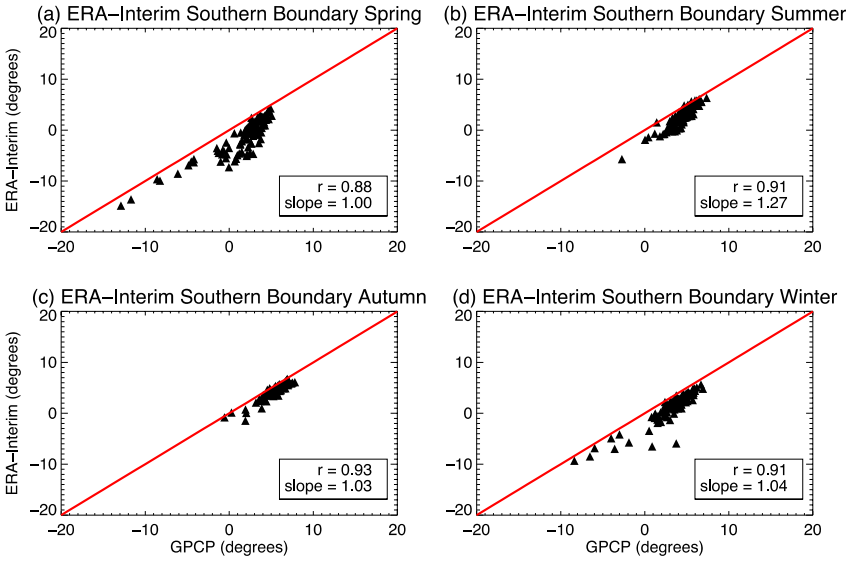

Figure 3.8: Same as in Figure 3.7, but for the southern ITCZ boundary.

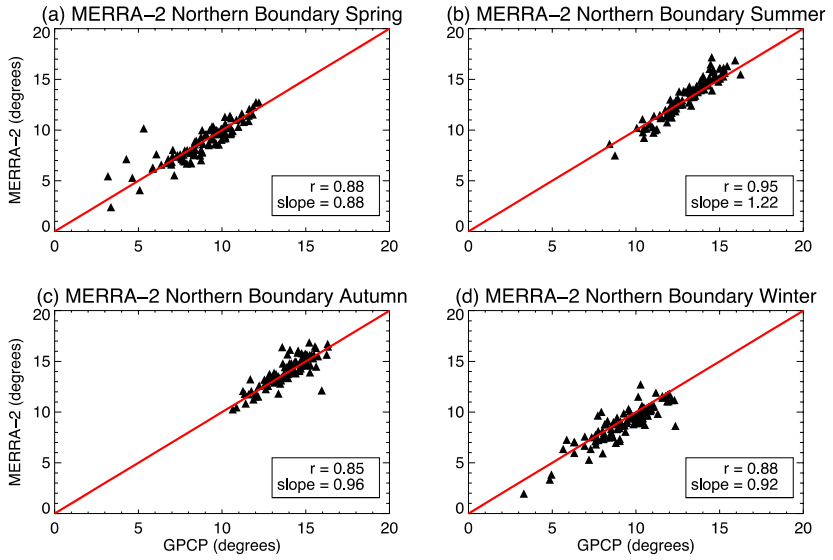

Figure 3.9: Seasonal comparisons of the northern ITCZ boundary location in MERRA-2 to GPCP.

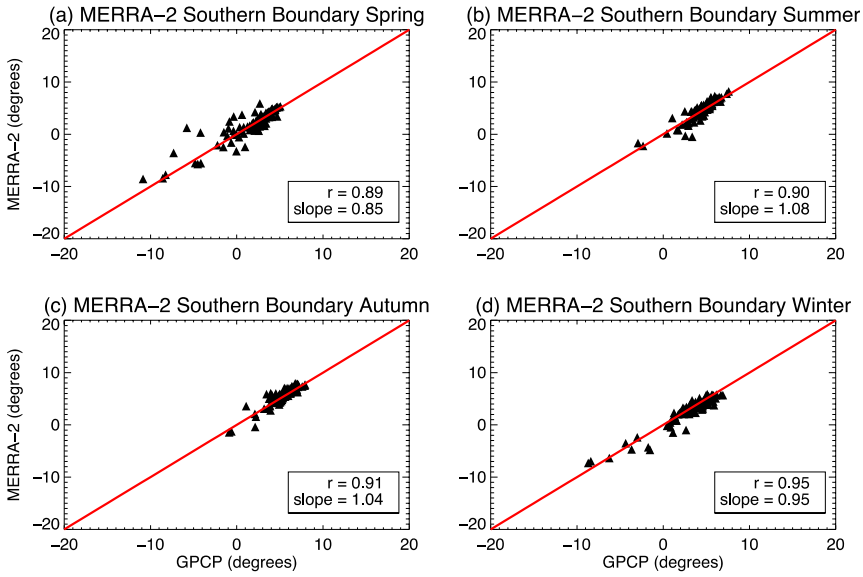

Figure 3.10: Same as in Figure 3.9, but for the southern ITCZ boundary.

The months with the lowest correlations between ERA-Interim and MERRA-2 were chosen and analyzed: April for the southern boundary and September for the northern boundary. Starting with the northern boundary, the rain rate difference in the September climatology is found and shown in Figure 3.11. MERRA-2 was subtracted from ERA-Interim since MERRA-2 has consistently agreed with GPCP. The decision was made to compare the reanalyses against each other in case more variables were to be analyzed that GPCP cannot provide such as wind components, relative humidity, or vertical motion.

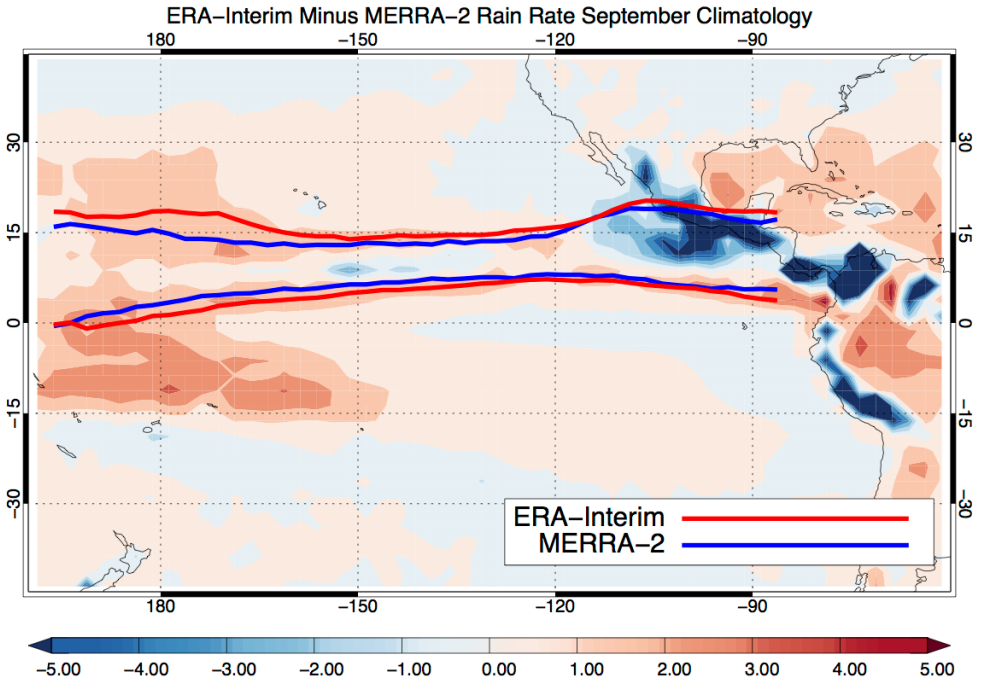

Figure 3.11: September rain rate climatology difference with respective ITCZ boundaries.

The rain rate differences are also analyzed for April in the same fashion. The rain rate difference in Figure 3.12, with MERRA-2 again being subtracted from ERA-Interim, shows that ERA-Interim again produces higher rain rates in the area between 15°S - 15°N over oceans. The northern boundary is again slightly more poleward in the ERA-Interim data set. The EPAC region in the September climatology showed higher rain rates for MERRA-2, but it is ERA-Interim in April. The northern boundary in the western portion of the CPAC region also shows higher rain rates in the ERA-Interim reanalysis and the ITCZ is slightly wider here as well. There is also no region in which

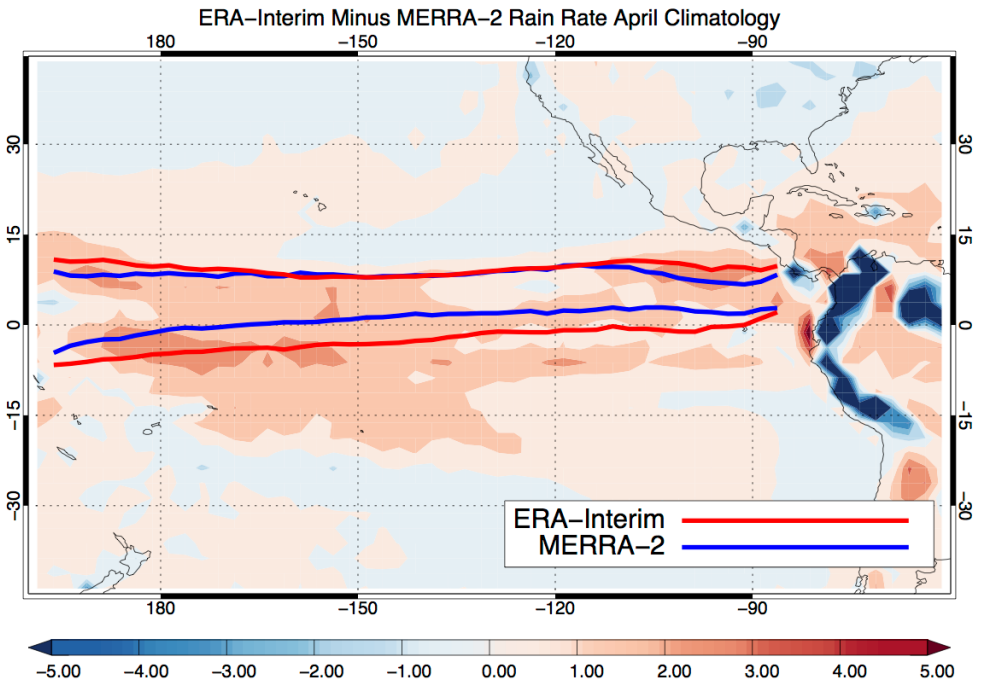

Figure 3.12: Same as in Figure 3.11, but for April.

the MERRA-2 southern boundary is more poleward or even the same latitude as ERA-Interim. Throughout most of the ITCZ, ERA-Interim places the southern boundary 3-4° further south than the MERRA-2 reanalysis. The CPAC region in particular has much higher rain rates in ERA-Interim for this month.

One of the potential explanations of the ERA-Interim tendency to place the ITCZ further south in the boreal winter/spring months could be due to the difference in dynamics between the EPAC and CPAC regions. The eastern region is dominated by the ITCZ while the western region has both the ITCZ and South Pacific Convergence Zone

(SPCZ). The SPCZ has been shown to be most northern during the North American winter (Zheng et al., 1997) and covers the most northern area during the spring months (Haffke and Magnusdottir, 2013). Figure 3.12 shows that ERA-interim places higher rain rates on average than either GPCP or MERRA-2 in the warm pool region, particularly in spring months. This implies that the heavy precipitation rates in the ITCZ are not adequately separated from the SPCZ placing the rain rate threshold, and therefore the southern ITCZ boundary, further south.

3.3 ITCZ Rain Rate Comparisons

Since the ERA-Interim reanalysis was shown to produce more rainfall near the SPCZ region, the rain rates in the ITCZ are analyzed. The top panel of Figure 3.13 is the GPCP rain rate climatology subtracted from MERRA-2 and the bottom is the GPCP rain rate subtracted from ERA-Interim. The plots show differing rain rate amounts between the three data sets with both reanalyses overestimating rainfall in the ITCZ and SPCZ region. These two plots show that there is an excess of precipitation in the CPAC region in general by the reanalyses which is likely contributing to differences in boundary locations, but it is also important to analyze how well the reanalyses agree with rain rate observations inside the bounds of the ITCZ.

Figure 3.14 is a collection of scatterplots of each reanalysis' longitude averaged rain rates on the ITCZ convergence center compared to GPCP. The rain rates at the center of the ITCZ in the ERA-Interim system are more intense on average, but particularly more intense when the rain rate is below 10 mm/day. When the same

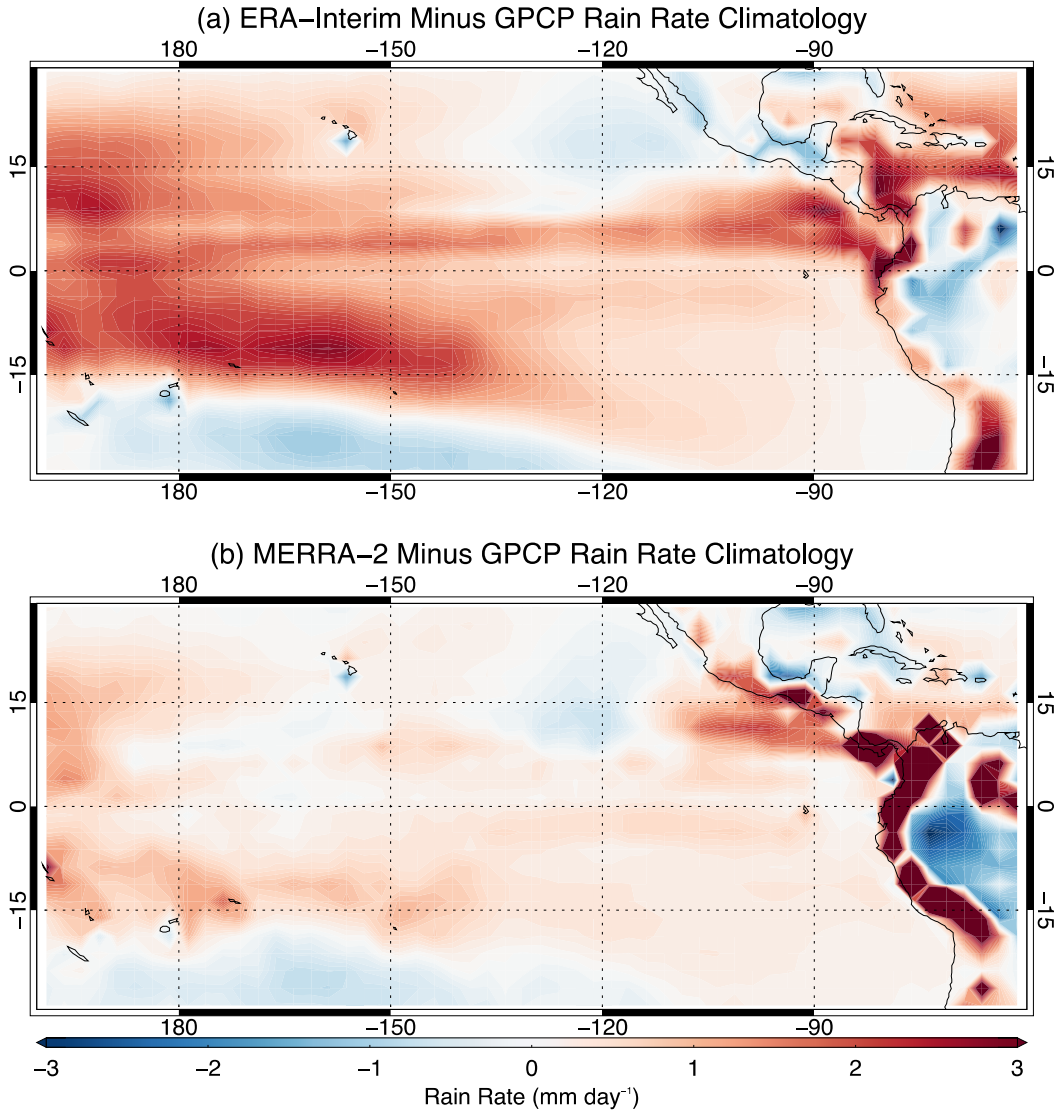

Figure 3.13: 35-year climatology (a) ERA-Interim and GPCP rain rate difference; (b) MERRA-2 and GPCP rain rate difference.

comparison is made between MERRA-2 and GPCP, there is no point where the rain rate is exclusively more intense in the MERRA-2 reanalysis. Furthermore, the ERA-Interim comparison struggles when rain rates at their lowest and highest which produces a

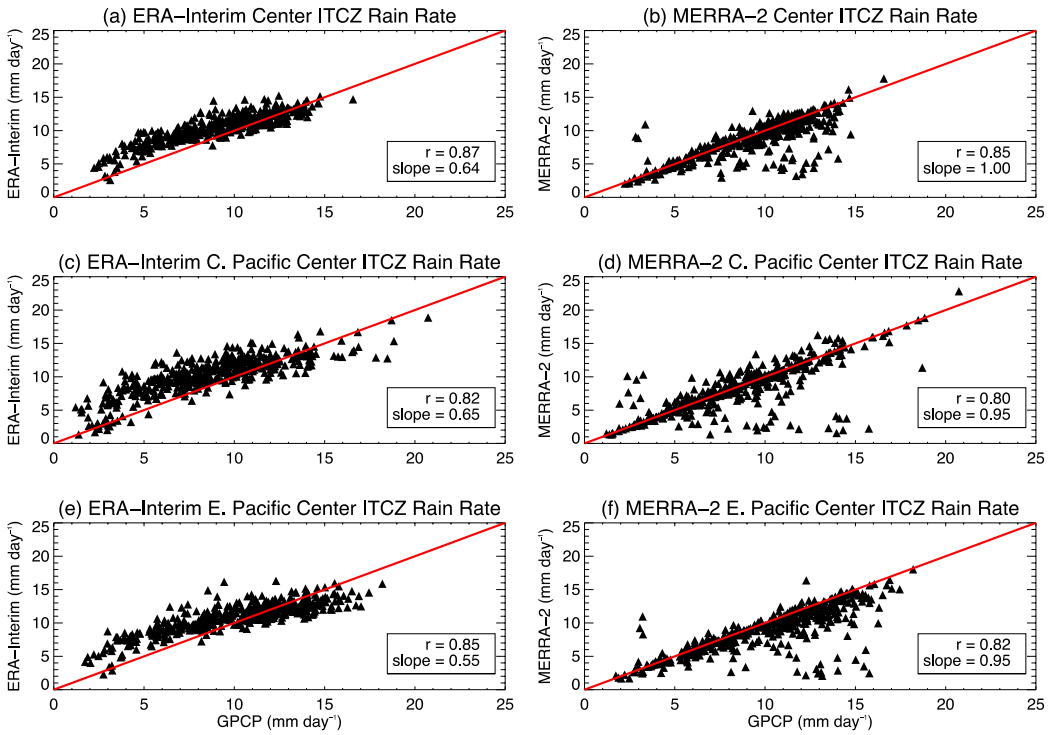

Figure 3.14 (a) and (b) Comparison of rain rate at the center of the ITCZ between the reanalyses and GPCP; (c) and (d) same, but for the CPAC region; (e) and (f) same, but for the EPAC region.

smaller slope. MERRA-2's rain rates produce a slope that is almost exactly one but shows significant spread as the rain rates get more intense with a tendency to underestimate at the highest rain rate.

Some of the issues shown with the center ITCZ rain rate are alleviated when the full ITCZ is considered. Figure 3.15 shows a collection of scatterplots when the meridional average of the rain rate within the ITCZ extent is taken and then averaged latitudinally over the full Pacific, EPAC, and CPAC regions. The correlations found in

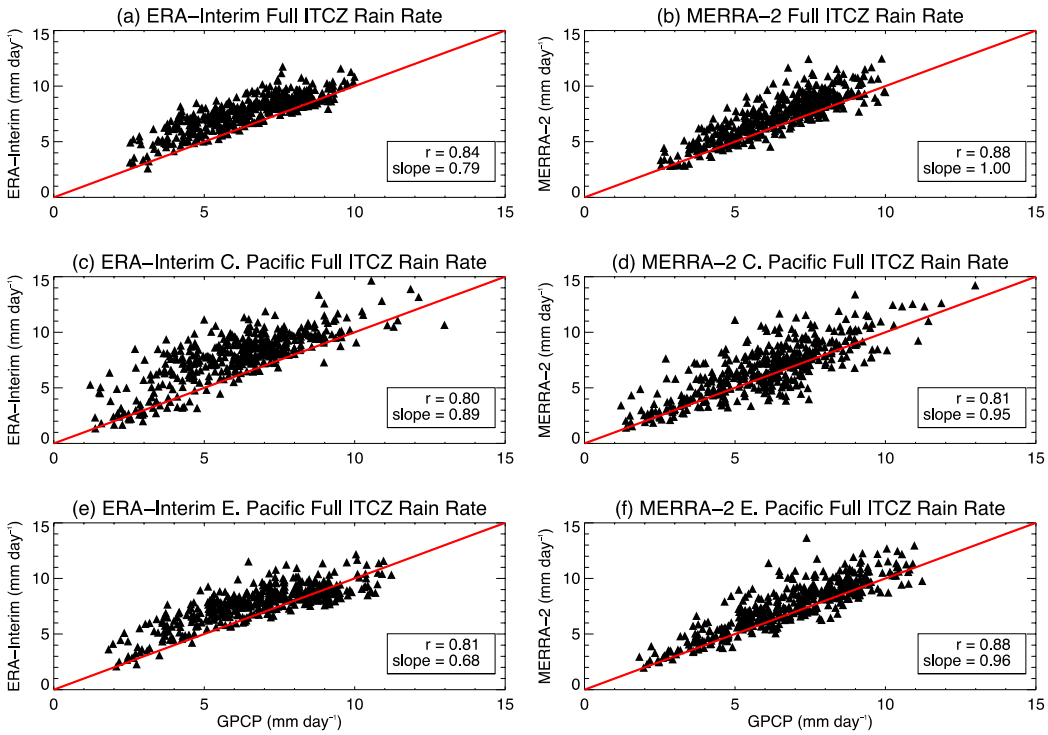

Figure 3.15: Same as for Figure 3.14, but rain rate for the full ITCZ.

Table 3.5 between ERA-Interim and GPCP do not change much, but the slopes get significantly closer to one and higher rain rates perform better. One significant difference when the full ITCZ is compared is that the CPAC region shows a majority of data points that are higher than GPCP. The MERRA-2 rain rates over the full ITCZ result in a larger spread of data when compared to GPCP, but the correlations remain high and the slope is still very close to one.

		CPAC ITCZ Center RR	CPAC Full ITCZ RR	EPAC ITCZ Center RR	EPAC Full ITCZ RR
ERA-Interim	Correlation	0.82	0.8	0.85	0.81
	Slope	0.65	0.89	0.56	0.68
	Intercept	4.65	2.47	5.31	3.14
MERRA-2	Correlation	0.8	0.81	0.82	0.88
	Slope	0.95	0.95	0.95	0.96
	Intercept	1.65	1.04	1.64	1.04

Table 3.5: Central and full ITCZ rain rate statistics when compared to GPCP.

3.4 Differences in Large-Scale Reanalysis Physics

The rain rate and ITCZ location discrepancies suggest broad differences in the large-scale physics. One of the objectives for this research was to determine the drivers behind any differences in ITCZ characteristics. Bosilovich et al. (2015) studied the differences between the MERRA and MERRA-2 reanalyses' variable fields by producing zonal average difference plots. The same method is applied here, with the domain restricted to the tropics (30°S - 30°N). The central Pacific is the region where the two reanalyses show the greatest disagreement, so it is chosen here for analysis.

Given that the rain rate climatologies between the two reanalyses were quite different, the first variable that was looked at was specific humidity. Studies have been conducted in warming climate models that imply a correlation between regions with increasing water vapor content and higher precipitation intensity (Allen and Ingram 2002; O'Gorman and Schneider 2009; Gastineau and Soden 2011). Given that ERA-

Interim tends to produce higher precipitation in the CPAC region, it is important to compare the water vapor between the reanalyses.

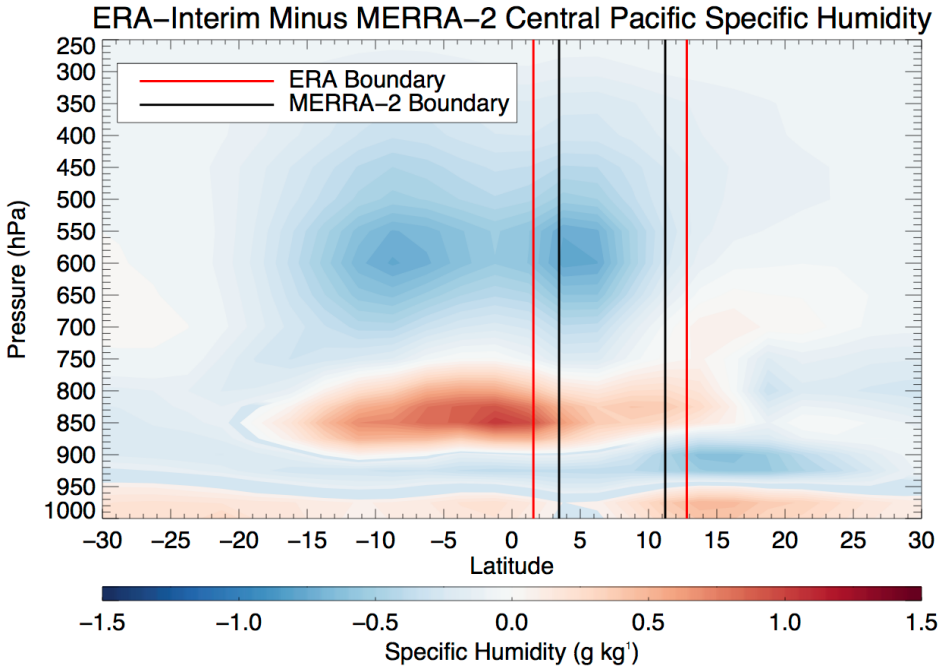

Figure 3.16: 35-year climatology specific humidity difference between the two reanalyses. The MERRA-2 climatology averaged over the central Pacific region is subtracted from ERA-Interim. The climatological ITCZ boundaries are overlaid, MERRA-2 in blue and ERA-Interim in red.

Figure 3.16 contains the climatological cross section of the MERRA-2 specific humidity subtracted from ERA-Interim over the central Pacific. The difference plot shows that the MERRA-2 reanalysis has a higher specific humidity throughout most of

the troposphere in the tropics. ERA-Interim shows greater specific humidity only very close to the surface and in the 900-700hPa levels between 10°S - 10°N. This area of higher water vapor is very significant, especially as it is in the same location as the inflated rain rates in ERA-Interim. More water vapor in this area may promote more deep convection in this area which may be a factor that contributes to more rainfall in ERA-Interim. This is an important difference, but we want to test how well other variables agree with MERRA-2 and if this is the only variable that contributes to higher rain rates in ERA-Interim.

The relative humidity and temperature fields are plotted in Figures 3.17 and 3.18, respectively. The temperature cross-section difference shows that the ERA-Interim central Pacific is warmer virtually everywhere below 600 hPa and cooler above which implies that it is more unstable on average than MERRA-2. As one might expect, the relative humidity difference closely mirrors the specific humidity difference between the reanalyses. This, again, does not quite explain the increased rainfall in ERA-Interim, especially near the ITCZ boundaries.

Figure 3.19 displays the central Pacific divergence plots as well as the difference in divergence between the two reanalyses. In the ITCZ region, the difference plot shows that MERRA-2 has stronger low-level (1000-850 hPa) convergence. From 850-400 hPa, the MERRA-2 ITCZ shows stronger divergence as well. Since divergence and upward motion are intrinsically related, the difference in ω is also plotted between the reanalyses (Figure 3.20). As implied by the divergence difference plot, the MERRA-2 ITCZ has stronger upward motion in the low-levels and stronger subsidence aloft. The more

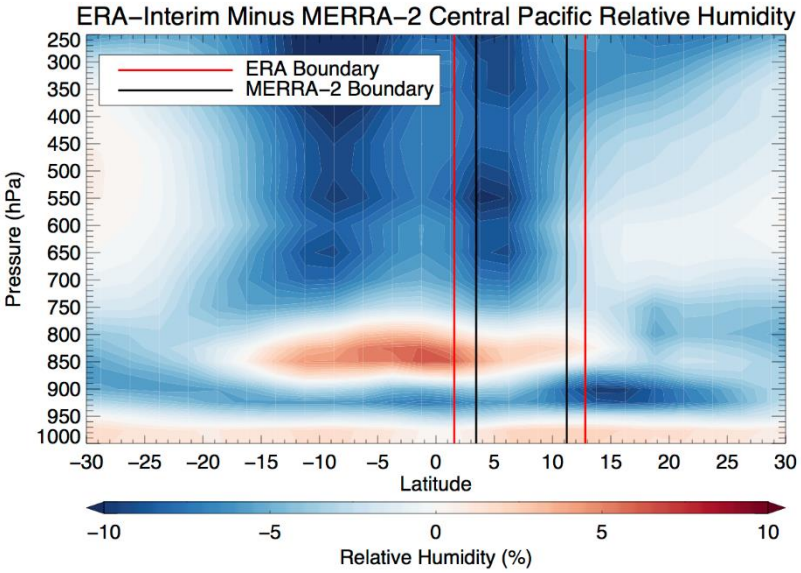

Figure 3.17: Same as in Figure 3.16, but for relative humidity.

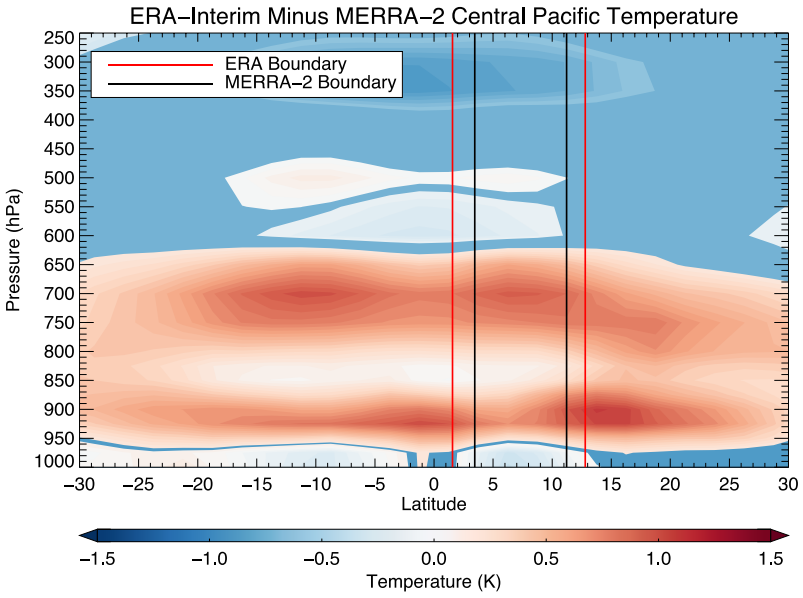

Figure 3.18: Same as in Figure 3.16, but for temperature.

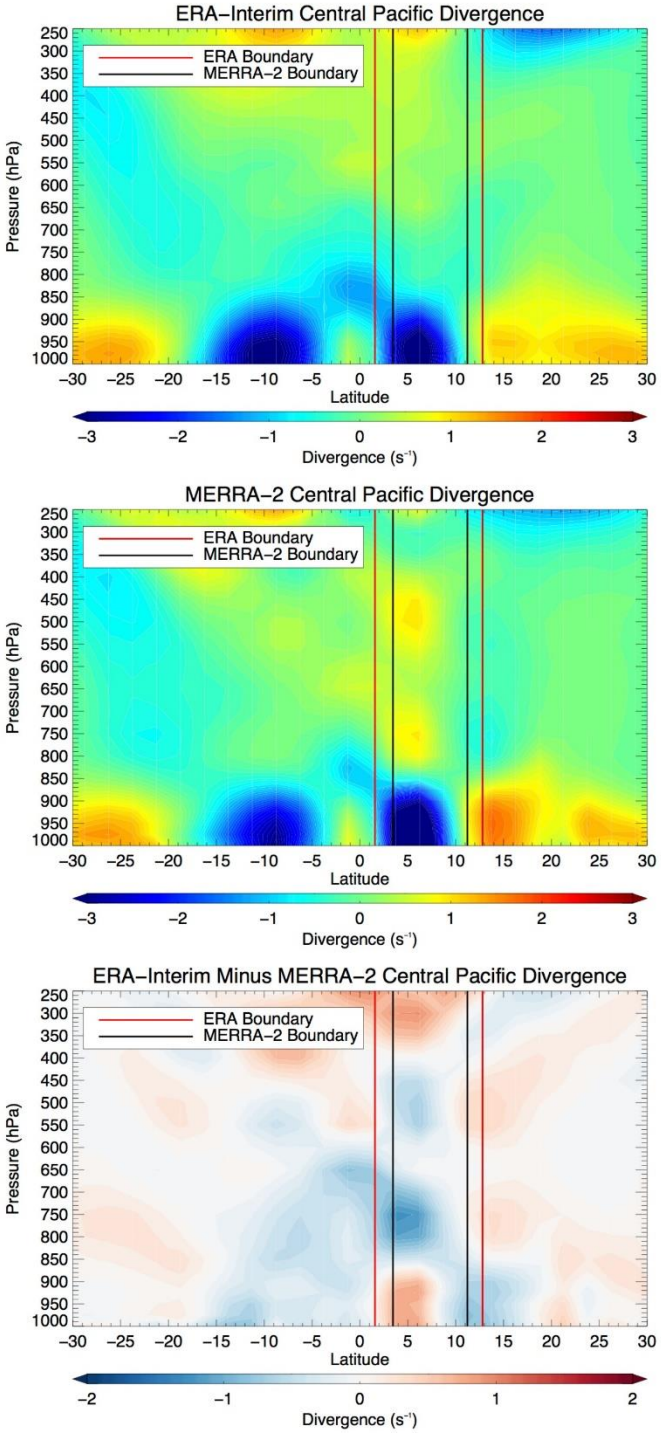

Figure 3.19: Comparison of central Pacific divergence fields with average ITCZ boundaries: ERA-Interim (red) and MERRA-2 (black).

important feature is that there appears to be stronger subsidence on either side of the ITCZ as well, particularly on the southern edge. From 15°S - 0°N, there is no location where MERRA-2 has stronger subsidence. And it is in exactly this area where there is much disagreement between the reanalysis-produced ITCZ boundaries.

High precipitation rates are expected from an area with strong low-level convergence and stronger upward motion as in the ITCZ. The ITCZ boundaries using this methodology are found using only precipitation rates, so any differences in modeling dynamics need to be identified. The most significant upward motion difference in the two reanalyses is in the mid-levels between 15°S - 0°. Figure 3.20 shows that ERA-Interim produces a broad area of upward motion with no zone of downward motion that would separate the ITCZ and SPCZ unlike MERRA-2 which presents a narrow separation between the two convergence zones. The enhanced rainfall produced from this region of broad ascent in ERA-Interim is the most likely reason for the breakdown of our methodology in the CPAC region. It is fair to say other methodologies such as the ω_{500} or the divergence methods would have also broken down in this region considering the difference in the dynamics between the reanalyses.

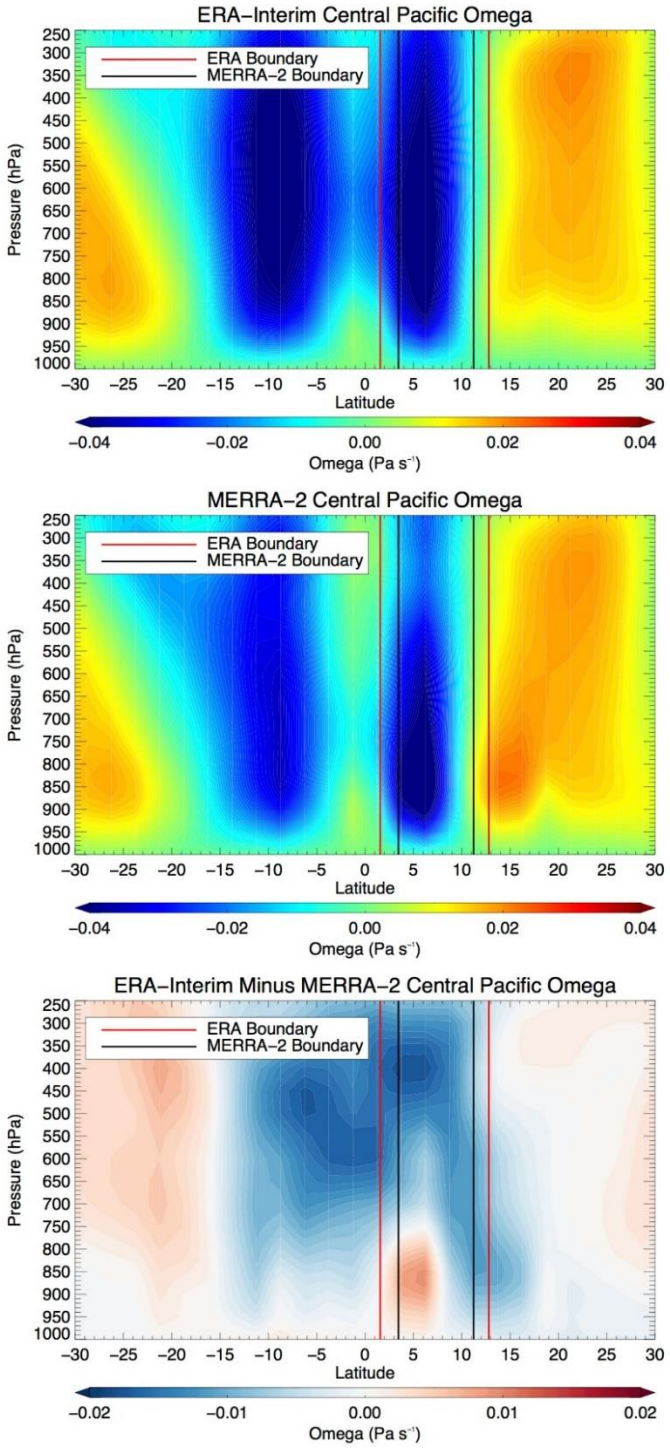

Figure 3.20. Same as in Figure 3.19, but for vertical pressure velocity.

3.5 Long-Term Trends

Although the data sets produce different ITCZ boundaries and rain rate intensities, the previous analysis in sections (3.1-4) suggests that the bias in ITCZ characteristics does not substantially vary as a function of width and intensity. This implies that the long-term trends may not be affected by the differences between the reanalyses once the data are deseasonalized. The long-term ITCZ metrics (extent and precipitation intensity) obtained from the reanalyses are compared against the satellite-retrieved results from previous studies.

Wodzicki and Rapp (2016) found a narrowing ITCZ in GPCP, particularly in the center Pacific region. The anomalies are calculated by removing the 35-year average monthly means from the rain rates and then plotting these results over the 35-year period. The full ITCZ width anomalies in Figures 3.21(a-b) and 3.22(a-b) reveal that the reanalyses capture the trend of ITCZ narrowing found in observations, but with varying success regarding the trend's magnitudes; Table 3.6 contains the full statistics found.

			Full Width Anomaly	North Extent Anomaly	South Extent Anomaly
GPCP	Slope	CPAC	-63.142	-16.294	-46.848
		EPAC	-43.544	-24.554	-18.990
ERA-Interim	Slope	CPAC	-54.221	-16.772	-37.450
		EPAC	-35.960	-17.331	-18.631
MERRA-2	Slope	CPAC	-61.073	-30.604	-30.470
		EPAC	-40.379	-15.431	-24.945

Table 3.6: ITCZ narrowing trends (km/decade) of the reanalyses' ITCZs.

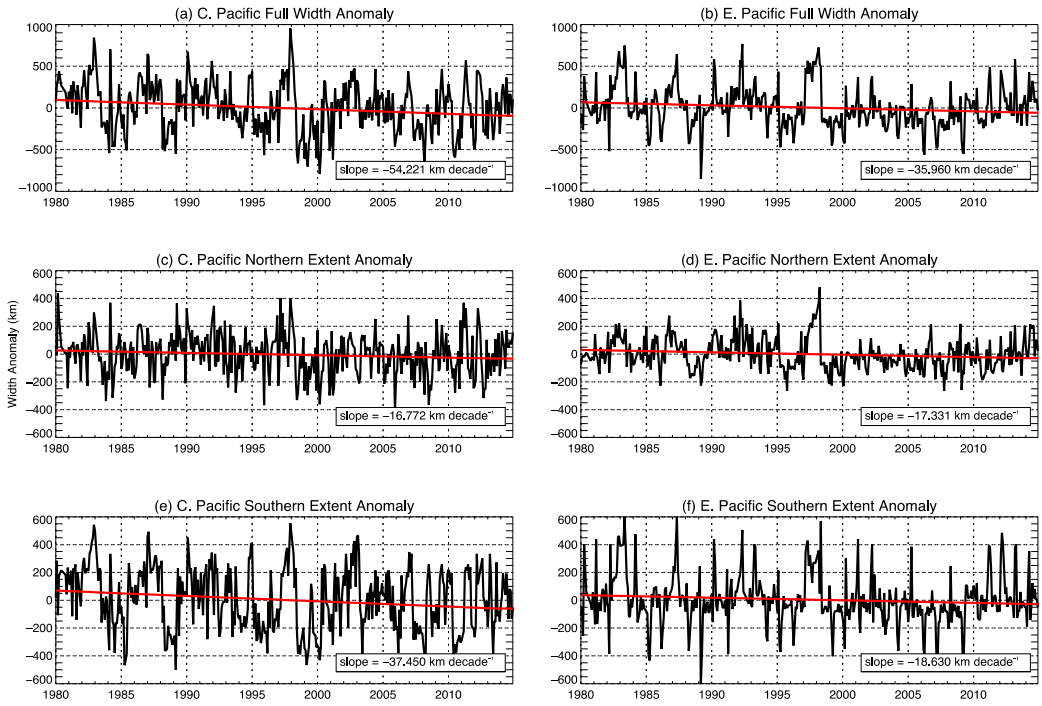

Figure 3.21: Reproduction of ITCZ width anomaly trends from Wodzicki and Rapp (2016) using ERA-Interim (similar to their Figure 5). (a) and (b) Full ITCZ width anomalies for ERA-Interim; (c) and (d) same, but for the northern ITCZ extent; (e) and (e) same, but for the southern ITCZ extent.

The findings from GPCP showed that the ITCZ narrowed more in the central Pacific region than in the eastern Pacific. Both the reanalyses were quite consistent with the magnitude of narrowing in both regions of the Pacific when compared to Wodzicki and Rapp (2016). The MERRA-2 reanalysis in particular is very close in both regions, but the full width anomalies are simply the sum of the northern and southern width anomalies. As such, it is possible that they could agree very well with the total narrowing of the ITCZ, but in the wrong portion of the ITCZ.

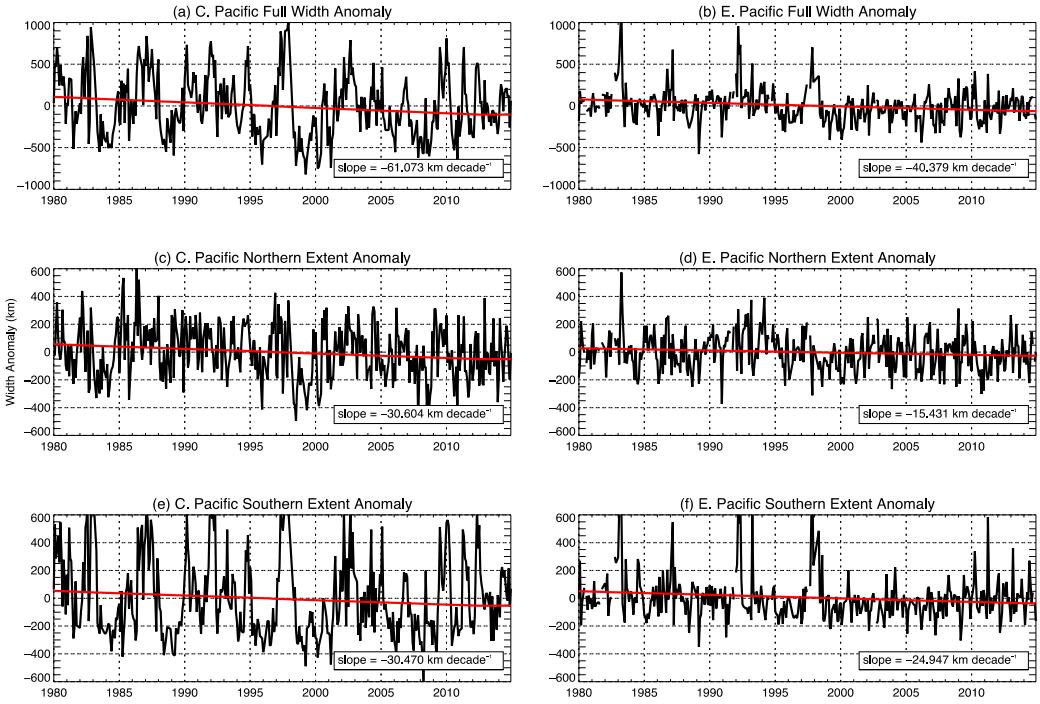

Figure 3.22: Same as in Figure 3.21, but for MERRA-2.

Figures 3.21(c-f) and 3.22(c-f) present the northern and southern width anomalies by region. The southern section of the ITCZ in the central Pacific is where the bulk of narrowing was found to occur according to results from GPCP. The northern ITCZ narrowed nearly twice as much the southern region of the central Pacific, which is more consistent with GPCP. The MERRA-2 ITCZ narrowed equally in the southern and northern portions. The north showed more narrowing than observations, but the south much less even though the total MERRA-2 width anomaly was closer to GPCP.

In the eastern Pacific, reanalyses show a slightly larger decrease in the southern ITCZ instead of the larger narrowing in the northern ITCZ found by GPCP. The eastern Pacific ERA-Interim ITCZ is shown to narrow almost equally in the north and south, but MERRA-2 shows significantly more narrowing in the southern ITCZ.

The ITCZ rain rate intensity was shown to increase over the time period of 1979-2014 by Wodzicki and Rapp (2016). The same time series analyses are presented for ERA-Interim and MERRA-2 in Figures 3.23 and 3.24 for the center and full ITCZ rain rate anomalies. The results show a consistent rain rate increase for each region of the Pacific in both reanalyses. The increased precipitation intensity found in Table 3.7 reinforces the trends by Wodzicki and Rapp (2016), but the magnitude of the trends for the reanalyses is different.

		CPAC ITCZ Center RR	CPAC Full ITCZ RR	EPAC ITCZ Center RR	EPAC Full ITCZ RR
GPCP	Slope	0.371	0.132	0.331	0.194
ERA-Interim	Slope	0.100	0.090	0.128	0.091
MERRA-2	Slope	0.323	0.162	0.620	0.387

Table 3.7: Rain rate trends (mm/day/decade) of the reanalyses' ITCZs.

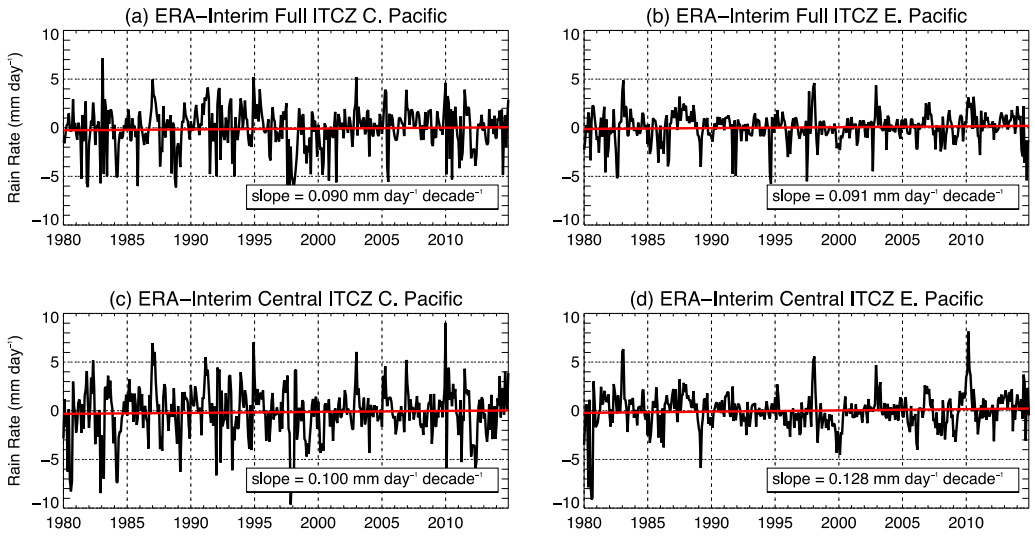

Figure 3.23: Reproduction of rain rate anomaly trends from Wodzicki and Rapp (2016) using ERA-Interim (similar to their Figure 6). (a) Full ITCZ rain rate anomaly trend in the CPAC region; (b) Full ITCZ rain rate anomaly trend in the EPAC region; (c) Center ITCZ rain rate anomaly trend in the CPAC region; (d) Center ITCZ rain rate anomaly trend in the EPAC region.

There is much disagreement in ITCZ metrics between the reanalyses and the satellite derived GPCP, but the long-term trends such as width and rain rate intensity are similar. The results also support previous findings of narrowing and rain rate intensification (Wodzicki and Rapp, 2016; Huang et al., 2013; Lau and Kim, 2015; Taylor et al. 2012; Su et al., 2017). The GPCP full ITCZ in the central Pacific had an increase in rain rate intensity, but not as large an increase as the rain rate in the ITCZ center. The ERA-Interim showed the same trends but the magnitudes of the increased rain rates were much less. The magnitudes of the increase are 50% less in the full ITCZ

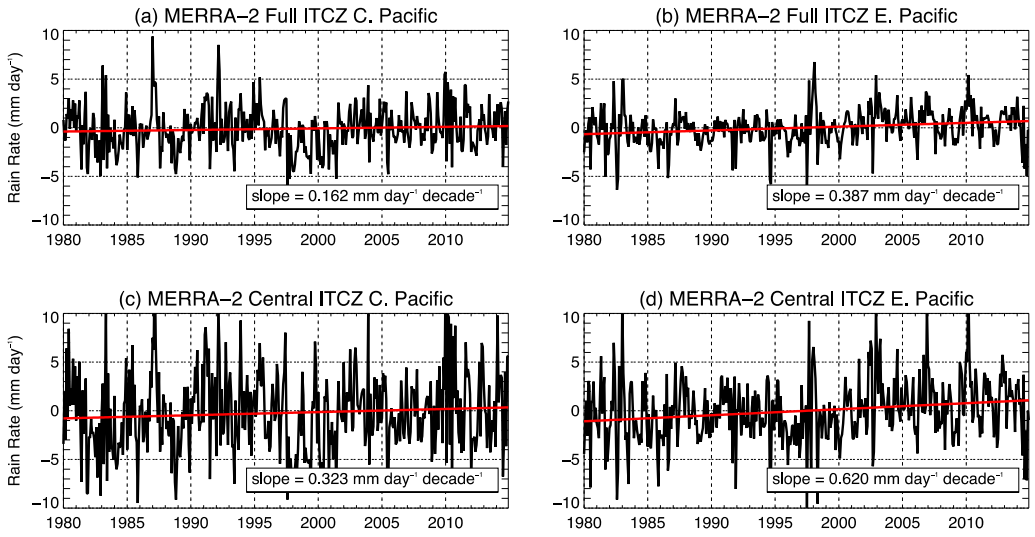

Figure 3.24: Reproduction of rain rate anomaly trends from Wodzicki and Rapp (2016) using MERRA-2 (similar to their Figure 6). (a) Full ITCZ rain rate anomaly trend in the CPAC region; (b) Full ITCZ rain rate anomaly trend in the EPAC region; (c) Center ITCZ rain rate anomaly trend in the CPAC region; (d) Center ITCZ rain rate anomaly trend in the EPAC region.

and nearly 75% less in the center of the ITCZ when compared to GPCP. The MERRA-2 results were nearly identical to GPCP for the full ITCZ, but overestimates intensification in the ITCZ center. Both reanalyses, regardless of magnitude, show a positive trend for rain rates in the ITCZ.

Figures 3.23 and 3.24 show the rain rate increases over the 35-year period in both regions of the Pacific as well. As in the CPAC region, the ERA-Interim rain rate increases underestimate the findings from GPCP. The opposite occurred when the MERRA-2 rain rate anomalies were plotted: these two results indicate an increase nearly

double that of GPCP. In both regions, the MERRA-2 rain rate anomalies are much more variable; some monthly anomalies can produce more than double the precipitation intensity of ERA-Interim or GPCP. In both reanalyses, the precipitation intensity increases over the 35-year period across the full Pacific. The two reanalyses have long-term trends consistent with observations regardless of their differing approaches to the physics near the ITCZ.

5. CONCLUSIONS

This study used atmospheric reanalyses to objectively identify the ITCZ and create a 35-year climatology of their characteristics including center, boundaries, and precipitation intensity. The method was adapted from the Berry and Reeder (2014) algorithm for monthly mean use by Wodzicki and Rapp (2016) and applied to gridded reanalysis and rain rate data sets to identify and compare ITCZ characteristics between different data sets. Dynamic and thermodynamic variables from each reanalysis were used to identify an ITCZ center and then reanalysis rain rates were used to define the ITCZ boundaries.

The characteristics found in the reanalysis-produced ITCZs largely agree with previous observational studies. The ITCZ tends to stay mostly in the northern hemisphere with the climatological mean center of 8° N (Waliser and Gautier, 1993; Bain et al., 2011). The annual meridional migration of the ITCZ is similar to those found in Bain et al. (2011), although the magnitude of the seasonal cycle differs between the reanalyses. The southern boundary location is shown to be more volatile than the northern boundary, which is most likely due to the reanalyses struggling to accurately depict the ITCZ/SPCZ relationship. The reanalyses, particularly ERA-Interim, are shown to produce differing rain rates near the ITCZ boundaries. This is consistent with studies that show these reanalyses have difficulty producing accurate rainfall over the Pacific (Dee et al. 2011; Bosilovich et al. 2017).

The reanalyses produce similar results for all ITCZ characteristics when compared to each other and to observational results found by Wodzick and Rapp (2016), with a few notable exceptions. The reanalyses calculate ITCZ centers that are highly consistent with each other, but ERA-Interim is shown to produce more poleward ITCZ boundaries than MERRA-2 or GPCP (Figure 3.6), so the boundaries were examined further. While the ERA-Interim ITCZ boundaries are wider throughout the year, disagreements are greatest mostly during the boreal autumn for the northern boundary and boreal spring for the southern boundary (Figures 3.7-10).

Because the boundaries are identified using a rain rate threshold, the rain rates between the three data sets were also compared to determine reasons for the differing boundary results. Climatologies for the two least correlated ITCZ boundary months (April and September) reveal the excess rain rate near southern ITCZ boundary's climatological location in the central Pacific (Figures 3.11-12). As noted by Bosilovich et al. (2017), the MERRA-2 also has excess rainfall in the SPCZ area compared to GPCP, but it is not as noticeable as ERA-Interim. This is not entirely surprising considering the assimilation scheme used by MERRA-2 uses a data set that shares many of the observation sites as GPCP (Gelaro et al. 2017). The increased precipitation rates in ERA-Interim near the intersection of the ITCZ and SPCZ appear to affect the southern boundary location because the rain rate threshold of 2.5 mm/day is further south on average. The large-scale physics near the excess rainfall was analyzed to ascertain what may be driving these precipitation differences in the central Pacific.

A correlation between regions with increasing water vapor content and higher precipitation intensity is implied by the literature (Allen and Ingram 2002; O'Gorman and Schneider 2009; Gastineau and Soden 2011). Humidity was found to have only slight differences between the reanalyses, but temperatures had significant differences. The entirety of the tropics in the ERA-Interim reanalysis is warmer throughout the depth of the lower troposphere and cooler above 500 hPa (Figure 3.18). This could promote more instability on average than MERRA-2 and perhaps account for some of the rain rate differences in the ITCZ.

The different ways the reanalyses handle the dynamics, particularly in the central Pacific, may also contribute to rainfall differences. The ERA-Interim reanalysis places such a broad region of ascending motion between 15°S - 0° that there is little separation between the SPCZ and ITCZ. The climatological rain rate difference between ERA-Interim and GPCP is largest in this warm pool area (Figure 3.13) and especially in the spring months when the SPCZ is furthest north. The increased rain rates in the CPAC region produced by ERA-Interim artificially drags the southern ITCZ boundary poleward and leads to a break down in the boundary identification methodology. Given the differences between reanalyses in the vertical velocity and divergence fields, it implies that other methodologies using these fields to define the ITCZ boundaries would have issues capturing the southern boundary as well.

The two reanalyses clearly display differences both in ITCZ characteristics and large-scale physics that drive the ITCZ, but the long-term trends show promising agreement with observations and those found in past studies (Huang et al., 2013; Lau

and Kim, 2015). The reanalyses show a unanimous agreement with ITCZ narrowing and intensification trends, but with differing magnitudes. MERRA-2 captures the full ITCZ rain rate intensification trends well, but tends to overestimate the center ITCZ rain rate intensification; ERA-Interim underestimates both rain rate intensification trends greatly, but still shows a steady increase. MERRA-2 shows a narrowing ITCZ for all categories, but tends produce equal narrowing in both the northern and southern portions of the ITCZ whereas ERA-Interim and GPCP agree that the southern ITCZ extent contracts the most. This was also shown by Bryne and Schneider (2016) using an assortment of CMIP5 models, but did not find a clear reason for the hemispheric asymmetry in the ITCZ narrowing.

GPCP is considered to be the most complete rainfall data set and is used as truth for this study, but it could have biases in the warm pool region of the Pacific given the lack of non-satellite measurements. In the far west Pacific, the automated methodology also has limitations since there are many months in all datasets where the rain rate threshold is simply not reached until latitudes so poleward that it is clearly not part of the ITCZ. ERA-Interim in particular struggles to identify adequate separation between the ITCZ and SPCZ regions. When using reanalysis rain rates, more care needs to be applied when identifying the ITCZ in the westernmost region of the Pacific. Since the methodology can break down in this region due to reanalysis-inflated precipitation, a secondary system might need to analyze when this is the case and use other criteria to place the ITCZ boundaries in a more realistic location. Two other methods were considered in Section 2.4 to deal with this issue, but neither methodology would have

provided better results than the simple rain rate threshold used in this study, but is still an issue that will need to be addressed in future work. This is also the only method of the three tested that can be directly compared to real world observations.

The reanalyses used to capture ITCZ characteristics compare well to observations, but should not be taken as truth. There is much work that needed to capture all aspects of the hydrological cycle in both reanalyses. Their shortcomings and biases are well known by their producers and are currently being improved (Dee et al, 2011; Bosilovich et al, 2017). The ITCZ itself needs further study if it is to be better understood. As the main driver of the ascending branch of the Hadley Cell in the Pacific, changes in the ITCZ could have global scale affects. The reanalyses have large differences both dynamically and thermodynamically to observations, yet managed to accurately capture the long-term ITCZ trends. More work is needed to definitively explain the drivers of the ITCZ variability and how they change over time. Future research may also use this automated algorithm on more GCMs and future editions of the reanalyses used here to more conclusively catalog ITCZ characteristics and compare them amongst more data sets. Future models and reanalyses will only continue to improve their accuracy which will provide valuable insight into the drivers causing changes in the ITCZ.

REFERENCES

Adler, R. F., G. J. Huffman, A. Chang, R. Ferraro, P.-P. Xie, and Coauthors, 2003: The version-2 Global Precipitation Climatology Project (GPCP) monthly precipitation analysis (1979-present). *J. Hydrometeor*., **4**, 1147-1167.

Allen, M. R., and W. J. Ingram, 2002: Constraints on future changes in climate and the hydrologic cycle. *Nature*, **419**, 224–232.

Asnani, G., 1968: The equatorial cell in the general circulation. *J. Atmos. Sci*., **25**, 133-134.

Bain, C. L., J. De Paz, J. Kramer, G. Magnusdottir, P. Smyth, and Coauthors, 2011: Detecting the ITCZ in instantaneous satellite data using spatiotemporal statistical modeling: ITCZ climatology in the east Pacific. *J. Climate*, **24**, 216-230.

Berry, G., and M. J. Reeder, 2014: Objective identification of the intertropical convergence zone: Climatology and trends from the ERA-Interim. *J. Climate*, **27**, 1894-1909.

Bjerknes, J., 1969: Atmospheric teleconnections from the equatorial pacific. *Monthly* Weather Review, **97**, 163-172.

Bosilovich, M. G., J.-D. Chern, D. Mocko, F. R. Robertson, and A. M. da Silva, 2015a: Evaluating observation influence on regional water budgets in reanalyses. *J. Climate*, **28**, 3631–3649.

Bosilovich, M. G., and Coauthors, 2015b: MERRA-2: Initial evaluation of the climate. NASA Tech. Rep. NASA/TM-2015-104606, Vol. 43, 136 pp.

Bosilovich, M. G., F. R. Robertson, L. Takacs, A. Molod, and D. Mocko, 2016: Atmospheric water balance and variability in the MERRA-2 reanalysis. *J. Climate*, **30**, 1177–1196.

Brown, P. J., and C. D. Kummerow, 2014: An assessment of atmospheric water budget components over tropical oceans. *J. Climate*, **27**, 2054–2071.

Byrne, M. P., and T. Schneider, 2016: Energetic constraints on the width of the intertropical convergence zone, J. Clim., **29**, 4709-4721.

Chou, C., and J. D. Neelin, 2004: Mechanisms of global warming impacts on regional tropical precipitation. *J. Climate*, **17**, 2688–2701.

Dee, D., S. Uppala, A. Simmons, P. Berrisford, P. Poli, and Coauthors, 2011: The ERA-interim reanalysis: Con_guration and performance of the data assimilation system. *Quart. J. Roy. Meteor. Soc*., **137**, 553-597.

Estoque, M., and M. Douglas, 1978: Structure of the intertropical convergence zone over the GATE area. *Tellus*, **30**, 55-61.

Fletcher, R. D., 1945: The general circulation of the tropical and equatorial atmosphere. *J. Meteor*., **2**, 167-174.

Frank, W. M., 1983: The structure and energetics of the east Atlantic intertropical convergence zone. *J. Atmos. Sci*., **40**, 1916-1929.

Gastineau, G., and B. J. Soden, 2011: Evidence for a weakening of tropical surface wind extremes in response to atmospheric warming. *Geophys. Res. Lett.*, **38**, L09706, doi:10.1029/2011GL047138.

Gelaro, R., and Coauthors, 2017: The Modern-Era Retrospective Analysis for Research and Applications, version 2 (MERRA-2). *J. Climate*, **30**, 5419–5454.

Gruber, A., 1972: Fluctuations in the position of the ITCZ in the Atlantic and Pacific Oceans. *J. Atmos. Sci*., **29**, 193-197.

Haffke, C., and G. Magnusdottir, 2013: The South Pacific convergence zone in three decades of satellite images. *J. Geophys. Res. Atmos.*, **118**, 10 839–10 849.

Holton, J. R., J. M. Wallace, and J. Young, 1971: On boundary layer dynamics and the ITCZ. *J. Atmos. Sci*., **28**, 275-280.

Huang, P., S.-P. Xie, K. Hu, G. Huang, and R. Huang, 2013: Patterns of the seasonal response of tropical rainfall to global warming. *Nat. Geosci*., **6**, 357-361.

Hubert, L. F., A. F. Krueger, and J. S. Winston, 1969: The double intertropical convergence zone-fact or fiction? *J. Atmos. Sci*., **26**, 771-773.

Huffman, G. J., R. F. Adler, D. T. Bolvin, and G. Gu, 2009: Improving the global precipitation record: GPCP version 2.1. *Geophys. Res. Lett*., **36**.

Lau, W. K., and K.-M. Kim, 2015: Robust Hadley circulation changes and increasing global dryness due to CO2 warming from CMIP5 model projections. *Proceedings of the National Academy of Sciences*, **112**, 3630-3635.

Levine, X. J., and T. Schneider, 2015: Baroclinic eddies and the extent of the Hadley circulation: An idealized GCM study, *J. Atmos. Sci*., **72**, 2744-2761.

Lin, R., T. Zhou, and Y. Qian, 2014: Evaluation of global monsoon precipitation changes based on five reanalysis datasets. J. Climate, **27**, 1271–1289.

Lu, J., G. A. Vecchi, and T. Reichler, 2007: Expansion of the Hadley cell under global warming. *Geophys. Res. Lett*., **34**.

Mitas, C. M., and A. Clement, 2006: Recent behavior of the Hadley cell and tropical thermodynamics in climate models and reanalyses. *Geophys. Res. Lett*., **33**, L01 810.

Mitchell, T. P., and J. M. Wallace, 1992: The annual cycle in equatorial convection and sea surface temperature. *J. Climate*, **5**, 1140-1156.

Neggers, R. A., J. D. Neelin, and B. Stevens (2007), Impactmechanisms of shallow cumulus convection on tropical climate dynamics, *J. Clim*., **20**, 2623–2642.

O'Gorman, P. A., and T. Schneider, 2009: The physical basis for increases in precipitation extremes in simulations of 21st-century climate change. *Proc. Natl. Acad. Sci. USA*, **106**, 14 773–14 777.

Pierrehumbert, R. T. (1995), Thermostats, radiator fins, and the local runaway greenhouse, *J. Atmos. Sci*., **52**, 1784-1806.

Riehl, H., and J. S. Malkus, 1958: On the heat balance in the equatorial trough zone. *Geophysica*, **6**, 503-538.

Rodell, M., and Coauthors, 2015: The observed state of the water cycle in the early twenty-first century. *J. Climate*, **28**, 8289–8318.

Seidel, D. J., Q. Fu, W. J. Randel, and T. J. Reichler, 2008: Widening of the tropical belt in a changing climate. *Nat. Geosci*., **1**, 21-24.

Stachnik, J. P., and C. Schumacher, 2011: A comparison of the Hadley circulation in modern reanalyses. *J. Geophys. Res*., **116**.

Su, Hui and Jiang, Jonathan H. and Neelin, J. David and Shen, T. Janice and Zhai, Chengxing and Yue, Qing and Wang, Zhien and Huang, Lei and Choi, Yong-Sang and Stephens, Graeme L. and Yung, Yuk L., 2017: Tightening of tropical ascent and high clouds key to precipitation change in a warmer climate. *Nat Commun.*, **8**, 15771.

Sun Q., Miao C., Duan Q., Ashouri H., Sorooshian S., Hsu K-L., 2018: A Review of global precipitation data sets: data sources, estimation, and intercomparisons. *Rev. Geophys*., **56**, 79-107.

Takacs, L. L., M. Suarez, and R. Todling, 2016: Maintaining atmospheric mass and water balance in reanalyses. *Quart. J. Roy. Meteor. Soc.*, **142**, 1565–1573.

Taylor, K. E., R. J. Stouffer, and G. A. Meehl, 2012: An overview of CMIP5 and the experiment design, *Bull. Am. Meteorol. Soc*., **93**, 485-498.
Uppala, M., and Coauthors, 2005: The Era-40 Re-analysis. *Quart. J. Roy. Meteor. Soc*., **131**. 2961-3012.

Waliser, D. E., and C. Gautier, 1993: A satellite-derived climatology of the ITCZ. *J. Climate*, **6**, 2162-2174.

Wang, C.-c., and G. Magnusdottir, 2006: The ITCZ in the central and eastern Pacific on synoptic time scales. *Mon. Wea. Rev*., **134**, 1405-1421.

Webster, P. J., 2004: The elementary Hadley circulation. *The Hadley Circulation: Present, Past, and Future*, H. F. Diaz, and R. S. Bradley, Eds., Kluwer Academic Publisher.

Wodzicki, K. R., and A. D. Rapp (2016), Long-term characterization of the Pacific ITCZ using TRMM, GPCP, and ERA-Interim, *J. Geophys. Res. Atmos*., **121**, 3153-3170.

Zheng, Q., X.-H. Yan, W. T. Liu, W. Tang, and D. Kurz, 1997: Seasonal and interannual variability of atmospheric convergence zones in the tropical Pacific observed with *ERS-1* scatterometer. *Geophys. Res. Lett.*, **24**, 261–263.